

# SafarDB: FPGA-Accelerated Distributed Transactions via Replicated Data Types

Javad Saberlatibari<sup>★</sup>, Prithviraj Yuvaraj<sup>★</sup>, Mohsen Lesani<sup>†</sup>, Philip Brisk<sup>\*</sup>, Mohammad Sadoghi<sup>‡</sup>  
University of California, <sup>\*</sup>Riverside, <sup>†</sup>Santa Cruz, <sup>‡</sup>Davis  
USA

## Abstract

Data replication is a critical aspect of data center design, as it ensures high availability, scalability, and fault tolerance. However, replicas need to be coordinated to maintain convergence and database integrity constraints under transactional workloads. Commutative Replicated Data Types (RDTs) provide convergence for conflict-free objects using relaxed consistency, and Well-coordinated Replicated Data Types (WRDTs) provide convergence and integrity for general objects using a hybrid model, relaxed when possible and strong when necessary. While state-of-the-art hardware acceleration of RDT uses Remote Direct Memory Access (RDMA), we observe that trends towards lower latency and higher throughput have driven recent data center architectures to leverage FPGAs as application accelerators. In contrast to deploying an FPGA-based Smart NIC, this paper connects an FPGA accelerator card directly to the network, which allows a complete redesign of the NIC to match the needs of the FPGA-hosted application. We co-design a network-attached FPGA replication engine with an FPGA-resident network interface, enabling near-network execution of replicated transactions and direct invocation of FPGA-resident operators. Following this approach, we introduce SafarDB, FPGA-accelerated Conflict-Free Replicated Data Types (CRDTs) and WRDTs. SafarDB accelerates both relaxed and strongly ordered replication paths; when strong ordering is required, SafarDB accelerates the underlying consensus control path. SafarDB improves CRDT latency and throughput by 7.0× and 5.3×, and WRDT latency and throughput by 12× and 6.8× compared to a state-of-the-art RDMA-based implementation. Further, experiments demonstrate that SafarDB is more resilient to crash-failures than existing CPU/RDMA-based CRDT and WRDT implementations, and, SafarDB can detect leader failures, and elect new leaders much faster than previously possible.

## 1 Introduction

Replicated Data Types (RDTs) are an object-level abstraction used inside replicated databases to implement distributed transactions that run on data center networks [21, 52, 83]. RDTs provide common abstractions, *e.g.*, registers, sets, and lists, by coordination strategies that guarantee convergence, availability, and integrity properties. Database systems use RDTs as building blocks for distributed transactions [30, 52, 64, 84] without requiring application developers to directly implement or interface with consistency models and coordination algorithms, or handling node and network failures.

We use RDT as a general category for replicated objects in transactional systems. Conflict-Free Replicated Data Types (CRDTs) are a subclass of RDTs whose operations commute, enabling relaxed consistency without coordination. Well-coordinated Replicated Data Types (WRDTs) extend this idea to support integrity constraints by

using relaxed execution when safe and invoking strongly ordered replication (consensus) only for operations that can violate integrity if reordered.

The objective of this work is to improve the performance of distributed transactions by accelerating RDT execution on network-attached FPGAs. The state-of-the-art RDTs are specialized for data centers equipped with RDMA networks [18, 41], which enable microsecond-scale remote memory access latencies. One study by Microsoft reports that RDMA traffic accounts for up to 70% of total network traffic in the Azure public cloud [9]. We observe that RDMA performance is limited by several sources of latency at each network node: PCIe transaction latency, and the use of host memory as an intermediary between the CPU and NIC; this complements recent research that has identified microarchitectural bottlenecks within RDMA NICs [77, 90]. Existing RDMA-based and RPC-based RDT systems largely assume CPU-hosted execution and are limited in (i) exploiting network-attached FPGA execution [3, 41, 62, 93], (ii) providing a true hybrid storage/execution model that partitions replicated state across FPGA memory and host memory under a single replication interface—beyond verb/protocol offload designs, [5, 85], (iii) efficiently supporting both relaxed and strongly ordered replication paths [3, 5], and (iv) inexpensively handling their failure control paths (*e.g.*, leader change/permission changes) [3, 41, 93].

To alleviate these bottlenecks, we propose SafarDB, an RDT design and implementation on network-attached FPGAs. SafarDB co-locates the RDT and NIC within the FPGA, using onboard memory sparingly. SafarDB specializes the NIC for communication between local and remote FPGA-resident accelerators, rather than supporting tens of thousands of concurrent threads running on the local CPU host. In doing so, we make a number of contributions that are fundamental to RDMA implementations for network-attached FPGAs and FPGA-based implementations of distributed systems:

- SafarDB augments the NIC with novel one-sided RDMA verbs that access integrated FPGA storage resources directly, and repurposes them to implement efficient Remote Procedure Calls (RPCs) to FPGA-resident accelerators.
- SafarDB provides FPGA-resident accelerators with direct access to the NIC’s microarchitectural state. SafarDB leverages this access to accelerate RDTs, which can use both relaxed and strong consistency models. In particular, it eliminates inefficiencies associated with leader election, a critical component of consensus.
- SafarDB provides a hybrid mode that utilizes the host CPU and its memory to scale capacity beyond the FPGA’s available memory, while maintaining a single replication/consistency interface across FPGA- and host-resident data (a challenge not addressed by prior FPGA-only designs)
- SafarDB reduces latency and increases throughput by 7.0×/5.3× for CRDTs shapiro11, calm (relaxed consistency), 12×/6.8× for

<sup>★</sup>Both authors contributed equally to this research.

WRDTs [40, 41, 63] (hybrid consistency: relaxed when safe, strong when necessary), and  $8 \times / 5.2 \times$  for YCSB [32]+ SmallBank [31] compared to state-of-the-art RDMA-based baselines.

We anticipate that this work will foment further investigation into distributed system deployment on network-attached FPGAs, especially for replicated transactional systems and database replication under a hybrid (FPGA+host) design model. FPGAs tend to obviate the distinction between application, operating system, and (micro)architecture: application and kernel functions can easily be co-located on a programmable FPGA fabric, with system calls reduced to wires between modules. SafarDB embodies this unification as a hardware-accelerated replication engine for transactional workloads, achieving higher performance than is otherwise unachievable as a result. Similarly, SafarDB demonstrates the benefits of customizing an FPGA-resident NIC to meet the needs of a transactional workload. We start with a NIC that provides one-sided RDMA verbs, which read from and write to onboard high-bandwidth memory. We then design and evaluate RDT-specific RPC mechanisms that eliminate otherwise spurious memory accesses. A similar approach can be applied to a wide variety of replicated databases and transactional workloads.

## 2 Preliminaries

### 2.1 Replicated Data Types (RDTs)

A *Replicated Data Type (RDT)* is a class of distributed objects that comprises a *data type* and a set of *transactions* (or method calls) [21]. Clients of an object can request transactions at any replica, and replicas coordinate them. Transactions may not necessarily execute in the same order across replicas. Thus, the states of replicas may *diverge* if replicas execute certain transactions in different orders. A *replicated execution is convergent* if all replicas reach the same state after all transactions are propagated and executed at all replicas. An RDT may include an *integrity or consistency invariant (as C in ACID)* [10, 11, 92], a predicate on its data that must be maintained between transactions. Examples of integrity properties include requiring that a bank account’s balance is always non-negative, or referential integrity in relational schema, *e.g.*, only a student registered at a university may enroll in a course.

Every transaction can be checked locally to be *permissible*, *i.e.*, preserve integrity at its issuing replica. We refer to this local invariant/precondition validation performed before executing a transaction as a *permissibility check*. However, when transactions are issued concurrently at different replicas and then propagated, they can become impermissible, *i.e.*, violate integrity in the target replicas. For example, suppose that two processes execute locally permissible withdrawal transactions from a bank account that ensures a positive balance; when propagated, the sum of the two withdrawals can overdraw the account. We say that a pair of transactions *convergence-conflict* and *integrity-conflict* if reordering them violates convergence and integrity, respectively. If either holds, we say that the pair conflicts. A transaction is conflict-free for convergence or integrity if there is no convergence or integrity-conflict with any other transaction, respectively. If both hold, we say that the transaction is conflict-free. An object is conflict-free if all its transactions are conflict-free. In order to preserve integrity, a transaction may be *dependent* on preceding transactions in the originating replica. For

example, a bank account withdrawal may depend on a preceding deposit to ensure a positive account balance. In order to preserve integrity, a remote replica must execute transactions only after transactions it depends on are already implemented. A transaction is dependence-free if it does not depend on any other transaction.

RDTs are implemented using a *consistency model*. *Strong consistency* (also known as State Machine Replication (SMR)), ensures convergence and integrity by imposing a linear ordering of transactions across replicas; this, however, limits responsiveness and availability [1, 2, 19, 20, 26, 53, 72, 88], which inhibits practical deployments [23, 27, 42]. *Relaxed consistency* models [68, 81] are more performant than strong consistency [55, 73], but guarantee convergence or integrity properties for a limited subset of RDTs. For example, *Convergent Replicated Data Types (CRDTs)* [52, 83] are convergence conflict-free RDTs, and can be implemented using relaxed consistency. CRDTs have been successfully used as building blocks for distributed applications, including distributed databases [52], key-value stores [30], online data stores [84], and collaborative editing [64]. We consider *operation-based CRDTs*. The appendix Table A.1 lists six CRDTs including register, and different types of counters and sets, which serve as our benchmarks; the Supplement describes each CRDT in greater detail. For example, increment and decrement on the counter type are conflict-free for convergence. We note that RDTs include a *query()* transaction, which reads values from the local object state; for brevity, we omit discussion of *query()*, except when needed.

*Well-coordinated Replicated Data Types (WRDTs)* [40, 41, 63] preserve both convergence and integrity, and are implemented using a hybrid consistency model [12–14, 29, 37, 57, 59–61, 86]: conflict-free transactions are implemented using relaxed consistency, and conflicting transactions are implemented using strong consistency. We will explain how WRDTs operate below. We note that WRDTs ensure convergence and integrity properties, whereas CRDTs only provide the former; CRDTs are a special case of WRDTs whose integrity predicate is the trivial assertion *true*.

WRDTs divide transactions into three mutually exclusive categories with increasing coordination cost: *reducible*, *irreducible*, and *conflicting* transactions. The first two are conflict-free. Reducible transactions are conflict-free, dependence-free, and summarizable. A transaction is *summarizable* if a sequence of invocations of that transaction can be aggregated into a single transaction. Summarizable transactions can be implemented efficiently: they can be aggregated at the local replica, and then a single transaction can be invoked at each remote replica to propagate the aggregated transaction. For example, the G-Counter contains a single non-negative value, *cnt*, initialized to zero. Each transaction *Increment(x)* adds  $x \geq 0$  to *cnt*; repeated transactions can be summed locally, and then the aggregate *Increment(cnt)* is propagated once to each remote replica. Irreducible conflict-free transactions are conflict-free but are either not dependence-free or not summarizable.

Conflicting transactions require strong consistency to ensure the same order of execution across all replicas. A set of transactions that conflict with each other should synchronize their orders; hence, they are called a synchronization group. Table B.1 (SG) lists the synchronization groups for each WRDT. As an example, consider the *Movie* WRDT for a movie theater system. *Movie* provides the transactions *addMovie*, *deleteMovie*, *addCustomer*, and *deleteCustomer*,

**Table 2.1: Average latencies measured for RDMA verbs on traditional and network-attached FPGA-based RDMA.**

	Read Latency	Write Latency
Traditional RDMA Network	1.8 $\mu$ s	2.0 $\mu$ s
Network-attached FPGA	0.0090 $\mu$ s	0.0089 $\mu$ s

which add and delete movies from a theater’s database, and reserve customer seats for movie showings. (The transactions *deleteMovie* and *addCustomer* succeed only if the given movie exists.) Since add and remove operations to a set convergence-conflict, the first two transactions are a synchronization group, and the other two transactions are another synchronization group. We will describe the State Machine Replication (SMR) implementation in subsection 4.4. Transactions of a synchronization group use the same instance of SMR [79].

The appendix Table B.1 lists five WRDTs that we adopted [29, 41] to serve as benchmarks in our experiments.

## 2.2 Remote Direct Memory Access (RDMA)

*Remote Direct Memory Access (RDMA)* allows user-space programs to access the memory of another node in a network without interrupting the remote CPU. State-of-the-art RDTs [41] and SMR protocols [3] are specialized for RDMA networks. While the RDMA standard specifies a wide variety of RDMA *verbs*, RDTs are implemented using Read and Write exclusively.

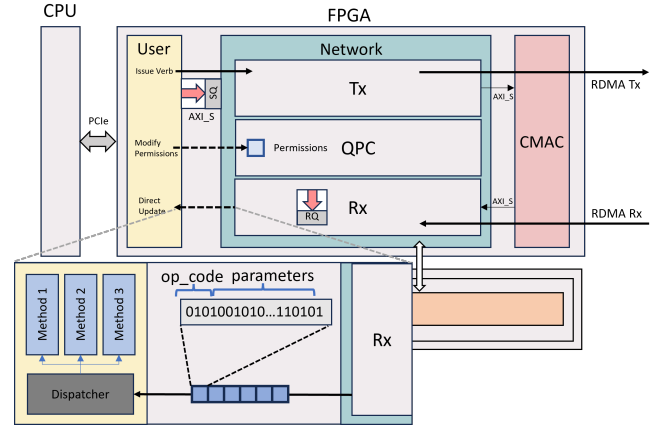
**Traditional RDMA.** The CPU, memory, and *RDMA-enabled NIC (RNIC)* are connected via PCIe. Local and remotely-accessible memory regions are allocated in user space. The *Queue Pair Context (QPC)* maintains a set of permissions which govern local and remote access to memory; applications may dynamically adjust permissions at runtime [3]. The CPU accesses a *doorbell register* via memory-mapped I/O to inform the RNIC when a verb is ready to transmit<sup>1</sup>.

**RDMA for Network-Attached FPGAs.** The FPGA card connects to a host CPU via PCIe, and features onboard *high-bandwidth memory (HBM)*. The host CPU programs and initializes the FPGA, initializes the internal state, and starts the FPGA execution. The *Ethernet Medium Access Control Block (CMAC)* and *Network* kernels implement a ‘soft’ RNIC, which supports RoCEv2, and communicate with the *application* kernel.

The application kernel and soft RNIC are connected via *AXI (Advanced eXtensible Interface) Streams (AXI\_S)*, and are connected to HBM via *Memory-Mapped AXI (MM-AXI)*. The RNIC QPs do not conform to the RDMA standard [85]. The send queue SQ is an AXI stream that is written by the application and is read by the Network kernel; the receive queue RQ resides in the Network kernel, and there is no completion queue CQ. Applications kernels communicate with the QPC to modify permissions. The supplement details the execution of FPGA-based one-sided RDMA verbs.

AXI-based communication within the FPGA is faster than PCIe. To quantify this, we generated 1 million random Read and Write requests on a traditional RDMA network and a network-attached FPGA cluster. Table 2.1 reports the average access latencies. Verbs implemented on the network-attached FPGA are two orders of magnitude faster than the traditional RDMA network.

<sup>1</sup>An expanded explanation is provided in the paper appendix: [github.com/javadsaberlatibari/FPGA\\_Consensus/blob/vldb\\_crfts\\_plus\\_kv/SafarDB-appendix-VLDB.pdf](https://github.com/javadsaberlatibari/FPGA_Consensus/blob/vldb_crfts_plus_kv/SafarDB-appendix-VLDB.pdf)

**Figure 1: FPGA-specific RDMA\_Write verbs enable RPCs.**

**RDMA vs. RPC** We observed that in a replicated execution, most of the data that remote replicas Write comprises transaction IDs and parameters, indirectly implementing *Remote Procedure Calls (RPCs)* via RDMA. RPCs exhibit orders of magnitude greater latency than RDMA verbs [17], and there have been successful proposals to reduce RPC overhead [46]. We show that network-attached FPGAs eliminate this disparity. In Figure 1, FPGA-specific Write verbs transparently enable RPCs that invoke FPGA-resident accelerators: the payload comprises a transaction ID (*opcode*) and parameters; a *Dispatcher* selects the appropriate accelerator, forwards the parameters, and invokes the accelerator.

## 3 SafarDB Overview

We first formalize the system settings and assumptions under which SafarDB operates.

**System Model.** We consider a distributed database deployed across  $N$  replicas. Each replica consists of a server equipped with a CPU and network-attached FPGA. Replicas communicate transactions<sup>2</sup> through RDMA over a reliable network.

**Network Model.** Replicas communicate via RDMA over Convergent Ethernet (RoCEv2). We assume reliable, in-order delivery of RDMA messages.

**Consistency Model.** SafarDB implements a hybrid consistency model based on Hamband [41]. Transactions are categorized into reducible, irreducible, and conflicting operations. Conflicting transactions require total ordering, and are serialized using a State Machine Replication (SMR) hardware module accelerating Mu[3], a primary-backup, RDMA-based consensus protocol which assumes one replica is designated as a leader, while the rest are considered followers. The leader performs coordination and commits transactions by writing into followers *replication log*, which is a circular buffer in memory.

**Fault Model.** We assume a crash fault model. A faulty replica may halt at any time and remain non-responsive thereafter, or return to functionality. Replicas are assumed to not exhibit Byzantine behavior. Both the leader and followers replicas can crash. When a follower crashes and comes back up, the leader can use the log for recovery by re-issuing the previously committed transactions to

<sup>2</sup>Transactions are assumed to be single-statement Transactions.

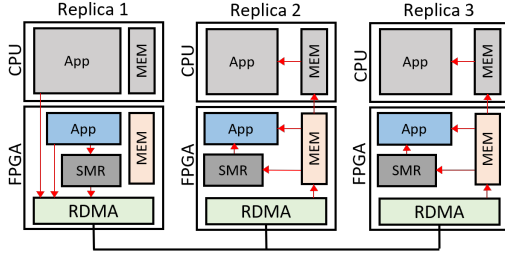


**Figure 2: SafarDB’s architecture stack: The red arrows depict the different paths transactions can take depending on the category of transaction.**

the newly returned follower. When a leader crashes, the remaining followers elect a new leader. Replicas crashes are detected by monitoring the *liveness* of replicas, which measure the activity and responsiveness of a replica.

**Architecture.** SafarDB is a distributed database connected through RDMA utilizing a network-attached FPGA accelerator that co-locates application logic, replication protocols, and RDMA networking on a single device to eliminate host-side RDMA overheads, and supports a hybrid execution model that supports a hybrid storage hierarchy including both host memory and device memory. It enables efficient implementations of CRDTs, WRDTs, and larger distributed applications and benchmarks, including YCSB and Small-Bank. SafarDB accelerates replication for the three categories of transactions: reducible, irreducible, and conflicting, explained in subsection 2.1. In addition to RDMA Read and RDMA Write verbs, we introduce and use FPGA-specific RDMA RPC verbs to further improve performance. The accelerator consists of multiple modules and memories on the FPGA, along with a CPU-resident application and CPU memory to expand the supported workload size.

Figure 2 provides the holistic picture of SafarDB. Transactions can originate from either the host CPU or FPGA, invoking the SMR module if total ordering is required *i.e.*, conflicting transactions. RDMA is used to propagate these transactions to other replicas. Receiving replicas can update FPGA and CPU data by reading from memory. For totally ordered transactions, SMR will read from memory and update the data.

Figure 3 depicts SafarDB’s accelerator in both FPGA-only and hybrid modes. The hardware modules on the FPGA consist of a CMAC kernel, which houses the 100G Ethernet Subsystem Xilinx IP used for Ethernet communication; a network stack that performs RoCEv2 RDMA operations; and a user kernel. The user kernel consists of a collection of user-specified operations for the FPGA-resident application, logic for the transactions, an SMR module, and the application’s data stored in on-chip BRAM. The FPGA also includes off-chip memory in the form of an 8 GB HBM buffer, which can be read from and written to via RDMA. On the CPU side, a CPU-resident application provides equivalent functionality to the FPGA-resident application in software, along with a shared memory buffer in main memory.

SafarDB can execute operations in an FPGA-only mode, where the entirety of the application state resides on the FPGA, or in a hybrid mode that allows the application state to be distributed between FPGA and CPU memory. Operations can be replicated to remote replicas from either the FPGA- or CPU-resident application using the three different transaction categories(see subsection 2.1).

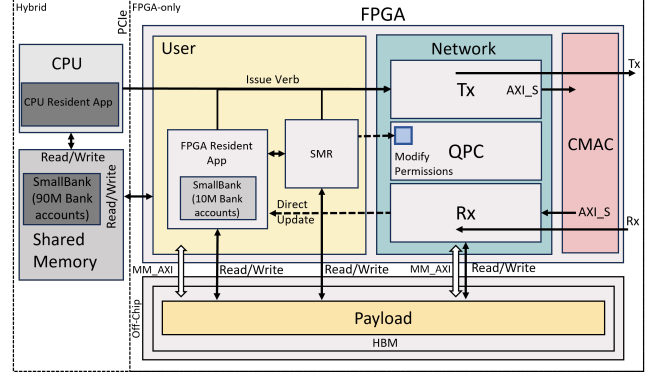


**Figure 3: SafarDB Architecture: SafarDB can operate in an FPGA-only mode, in which the data is stored entirely on the FPGA. It can further operate in hybrid mode, in which the CPU memory is used to store additional data.**

Conflicting transactions are totally ordered and use a dedicated SMR module, explained in subsection 4.4.

In FPGA-only mode, SafarDB is limited by the memory available on the FPGA. However, because the application resides on the same fabric as the RDMA network stack, RDMA operations are extremely fast. This is achieved by replacing PCIe communication with the Advanced eXtensible Interface (AXI) protocol, a lightweight synchronous on-chip communication protocol. In order to execute a reducible transaction, the FPGA-resident application issues a local update to its on-chip BRAM, and then issues an RDMA Write, which travels through the network module on the transmit path, exits through the CMAC kernel, and reaches the receiving replicas’ memory. The replicas then read from HBM memory to update their local data. In order to execute a conflicting transaction, the FPGA-resident application forwards the transaction to SMR for total ordering. SMR performs a round of consensus, and commits the totally ordered operation into the replicas’ logs in HBM. The replicas, similar to the reducible case, are responsible for retrieving the value from memory.

**Design Principle # 1:** In traditional RDMA systems, the CPU running the host application issues RDMA verbs to the RNIC via PCIe, incurring communication overhead. By collocating the application and RNIC hardware on a single FPGA chip, PCIe communication overhead is replaced by lightweight on-chip communication, and near-network processing is enabled.

SafarDB provides the hybrid mode for cases where the entire dataset cannot fit within the FPGA memory. In this mode, the FPGA performs transactions on FPGA-resident data. Additionally, the CPU can perform transactions by either issuing RDMA operations directly to the network module through PCIe or by triggering SMR to perform consensus for conflicting transactions. On the receiving side, after reading from the HBM memory, a dedicated module writes to host memory to update the CPU-resident data.

## 4 RDT Acceleration in SafarDB

In this section, we present in-depth explanations of how SafarDB implements the three categories of transactions, their optimizations, and a detailed description of the hardware implementing SMR.

#### 4.1 Reducible Transactions

SafarDB implements three configurations for reducible transactions. They use the RDMA Write and SafarDB’s custom RDMA RPC verbs. For example, let the system comprise  $N$  replicas, and the replicated data comprise one scalar  $B$ .

(1) RDMA Write (no buffer): Each replica allocates an  $N$ -element array,  $A$ , in the HBM memory. The element  $A[i]$  is written exclusively by the  $i^{th}$  replica, and is read locally. The  $i^{th}$  replica summarizes its scalar into a single value, and RDMA Writes that summary to  $A[i]$  at all remote replicas. At each remote replica, the next data access updates  $B$ .

(2) RDMA Write (with buffer): A copy of  $A$  is allocated within the FPGA in addition to HBM memory. Replicas RDMA Write summaries to  $A$  in memory. In the background, the replicas periodically poll memory to update the FPGA-resident copy of  $A$ . The next data access updates  $B$  from the FPGA-resident copy of  $A$  without accessing memory.

(3) RDMA RPC: Reducible transactions are propagated as RPCs to remote replicas (Figure 1), eliminating array  $A$ .

**Example.** In Figure 4a, assume the system comprises  $N$  replicas implementing a Bank Account with a balance  $B$  with a reducible transaction  $deposit(x)$ , which can increment balance  $B$  by  $x$ . Each replica allocates an  $N$ -element array,  $A$ , where  $A_i$  is the  $deposits$  of replica  $i$ . When replica  $i$  executes  $deposit(x)$ , first its local  $B$  is incremented by  $x$ , then  $B + x$  is written into the remote replicas’ memory at  $A_i$  (through  $a$ ), overwriting the previous values. In configuration (1), when the remote replica needs to read the total balance  $B$  it will read from memory (through  $b$ ) and combine all replica balances. In configurations (2), a background module pulls the remote balances from memory (through  $c$ ) so when the balance is required, only fast on-chip BRAM is read. In configurations (3), the remote replicas on-chip BRAM are directly updated from the network (through  $d$ ); removing the need to poll memory.

#### 4.2 Irreducible Conflict-free Transactions

SafarDB implements irreducible conflict-free transactions using RDMA Write and SafarDB’s custom RDMA RPC verbs. For example, let the system comprise  $N$  replicas, and each replica’s data comprises of a set  $S$ .

(1) RDMA Write: In Figure 4b, each replica allocates  $N$  queues in memory, where  $Q_i$  is written exclusively by the  $i^{th}$  replica and is read locally. The  $i^{th}$  replica locally updates  $S$ , and propagates the transaction to remote replicas by RDMA Writing the opcode to  $Q_i$  (through  $a$ ). The remote replica periodically polls the queues by issuing memory reads (through  $b$ ), and updates  $S$ .

(2) RDMA RPC: In Figure 4b (c) Irreducible conflict-free transactions are propagated as RPCs to remote replicas (Figure 1), eliminating queues and memory reads (through  $c$ ).

**Example.** In Figure 4b, assume the system comprises  $N$  replicas implementing a Course management system with a set of students  $S$  with an irreducible transaction  $addStudent(x)$ , which appends student  $x$  to  $S$ . Each replica allocates  $N$  queues, where  $Q_i$  is the transactions performed by replica  $i$ . When replica  $i$  executes  $addStudent(x)$ , first it locally appends  $x$  to  $S$ , then appends the transaction to  $Q_i$  in remote replicas (through  $a$ ). In configuration (1), a background module polls the remote queue to apply the outstanding  $addStudent(x)$  transaction (through  $b$ ) to the on-chip

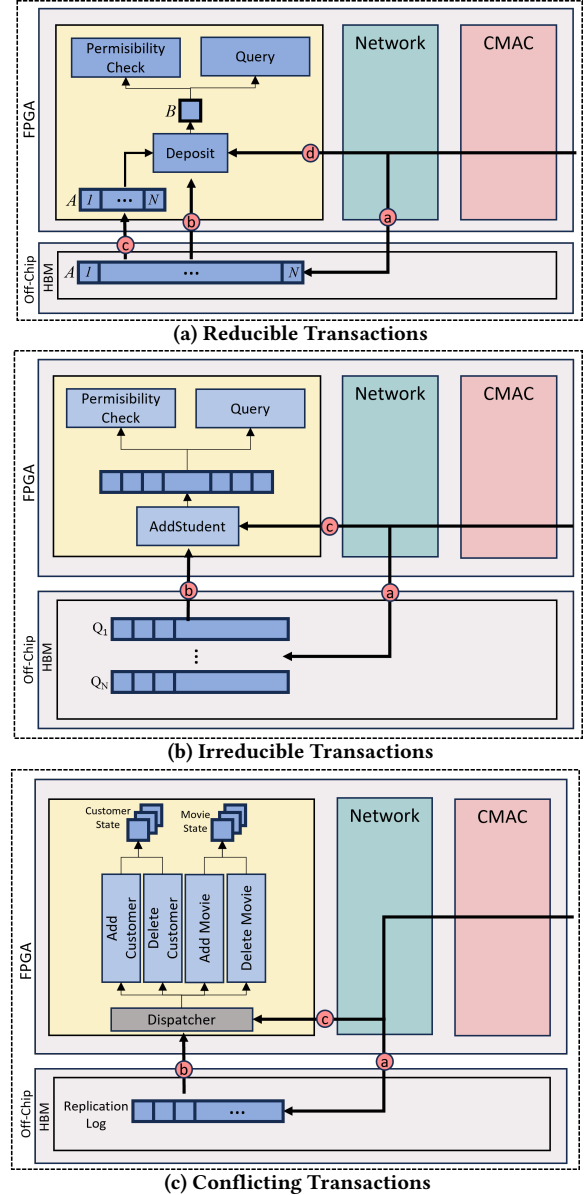


**Figure 4: The implementation of the three transaction categories.**

BRAM set  $S$ . In configuration (2), the remote replicas on-chip set  $S$  is directly updated from the network (through  $c$ ), removing the need to poll memory.

#### 4.3 Conflicting Transactions

SafarDB implements conflicting transactions using (a) RDMA Write verbs and (b) a new RDMA RPC Write-Through verb. For example, consider a system with  $N$  replicas, and each replica’s data comprises of a set  $S$ . Conflicting transactions require synchronization by an SMR protocol (see Figure 5). Each synchronization group maintains an instance of SMR, and each conflicting transaction invokes replication on the SMR of its synchronization group. We subsequently describe SMR in subsection 4.4.

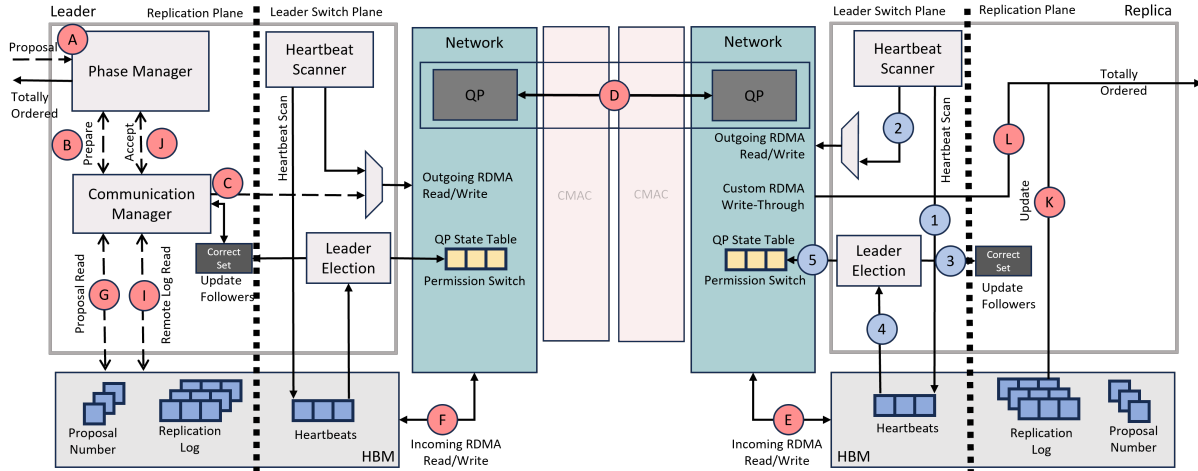


**Figure 5: SMR in SafarDB: The solid lines represent the portions of the SMR that operate regardless of leader status and the dashed lines represent the leader-specific operations.**

Each replica allocates a *replication log* in memory. Each replication log entry is a pair of values: a proposal number and operation. The proposal number ensures total ordering, and an operation consists of an opcode, which identifies the conflicting transaction to execute, and input parameters for the transactions. The replication log is used to buffer committed transactions as well as for recovery. We consider that the replication log can grow beyond the capacity of FPGA-integrated storage; therefore, it is allocated in memory.

(1) RDMA Write: In Figure 4c, RDMA Writes propagate conflicting transactions to remote replicas by appending them to the replication log. The replica repeatedly polls the log to identify newly-appended transactions as soon as they are written. New transactions are read and invoked via the Dispatcher. Accesses to *S* read the log and execute any conflicting transactions that are present, ensuring that the state is up-to-date.

(2) RDMA RPC Write-Through: In Figure 4c, conflicting transactions are propagated as RPCs to remote replicas (through *c*) and are simultaneously appended to the replication log (through *a*). The RPC does not access the replication log; however, the log is updated to support failure recovery.

**Example.** In Figure 4c, assume the system comprises  $N$  replicas implementing a Movie ticking system with a set of movies  $M$  with conflicting transactions  $addMovie(x)$ , and  $deleteMovie(x)$ , which append and pop movie  $x$  from  $M$ , respectively.  $addMovie(x)$ , and  $deleteMovie(x)$  are dependent each other, therefore form a synchronization group (see subsection 2.1). Each replica allocates replication log, in memory, per synchronization group (see subsection 4.4). When a replica executes  $addMovie(x)$ , first it triggers its SMR module, which performs a round of consensus, then commits the transaction locally then replicates it to other replicas by appending the replication log (through *a*). In configuration (1), the replica will poll the replication log for committed transactions (through *b*), also polling the log when the  $M$  accessed to ensure the most up to date data. In configuration (2), the SMR module uses the custom RPC to both append the replication log (through *a*), and directly updates the FPGA-resident data (through *c*).

**Design Principle # 2:** RDMA-based communication requires receiving replicas to access memory, incurring memory access latency. Although buffering and background polling can mitigate this overhead, direct updates enabled by custom RDMA RPC verbs can eliminate the access entirely.

#### 4.4 Accelerated Consensus

SafarDB provides strong consistency for conflicting transaction through an FPGA-accelerated implementation of Mu [3] (Figure 5) an RDMA-based SMR protocol for the crash-failure model: a replicas either crashes and stops, or executes correctly. The SMR picks a replica as the leader, with the remaining replicas designated as followers. Functionality is partitioned between two planes, a *Replication Plane* and a *Leader Switch Plane*, described in the following subsections.

**Replication Plane.** In the *Propose* phase, a new leader confirms the follower list by obtaining write permissions from a quorum (majority) of replicas, and then proposes a new transaction (at A). After transitioning into the *Prepare* phase (at B), the leader RDMA reads the latest proposal numbers from followers (through C, D, E, F and G). The leader RDMA writes the next highest proposal number to the followers (through C, D, E). It then RDMA reads each follower’s log slot that it intends to write (through C, D, E, F and I). If all followers’ log slots are empty, the leader proceeds to the *Accept* phase with its own transaction. If the leader reads a non-empty log slot, then that follower previously committed a different conflicting transaction; if so, the leader adopts that transaction instead. If multiple follower slots are non-empty, the leader adopts the transaction from the slot with the highest proposal number.

In the *Accept* phase (at J), the leader executes the conflicting transaction and RDMA writes it to the followers’ replication logs (through C, D, E). Followers read their logs (at K) and execute the transaction. If the originally proposed transaction was executed, the leader restarts from the first phase to prepare for the next conflicting transaction; if not, the leader repeats the *Prepare* phase for the originally proposed transaction.

With custom RDMA verbs, the final RDMA write in the *Accept* phase is replaced with RDMA RPC write-through. Thus, the application states for the followers are directly updated from the

network (at L). The followers no longer need to read their logs (at K) although their logs are updated (through C, D, E), similarly to traditional RDMA write.

**Leader Switch Plane.** The leader of SMR may fail. In order to maintain liveness, replicas need to detect leader failure when it occurs and elect a new leader. Each replica stores an array of *heartbeats* in memory, one for each other replica. Each heartbeat is an RDMA-exposed incrementing counter that allows the replica to express its liveness for a remote replica.

Each replica’s *Heartbeat Scanner* periodically increments its heartbeats (Figure 5 at 1), and RDMA Reads heartbeats of remote replicas (through 2, D, F, E, 4). If a remote replica’s heartbeat is constant after several reads, then the replica is assumed to have failed, and it is removed from the set of correct replicas (at 3).

If a leader is thought to have failed, then a new leader is elected: the live replica with the smallest ID. Leader operation relies on RDMA QP connections (subsection 2.2). The QP state is *open* or *closed*; RDMA Writes to a closed QP fail. Each follower has one open QP that grants write permission to a leader. If a follower determines that a leader has failed, it closes its QP with the leader, and then opens a new QP with the new leader (at 5).

Changing Leaders in this manner is called a *Permission Switch*. The fastest way to switch permissions is to change QP access flags; however, doing so while RDMA verbs are in-flight may induce a QP error. Software Mu [3] implements a fast path when no error occurs, and a slow path which detects and recovers from errors; only the slow path modifies the QP state. In a traditional RDMA network (subsection 2.2), modifying RDMA write permissions takes hundreds of microseconds, accounting for ~30% of fail-over time. The developers of Mu attribute this overhead to the lack of hardware optimization in the RNIC and its interface [3], which points to PCIe round-trip latencies. In our networked-attached FPGA (subsection 2.2), the SMR kernel can access the QP state directly.

**Design Principle # 3:** Changing RDMA permissions can take hundreds of microseconds. By colocating Mu and RNIC hardware on a single FPGA chip and exposing internal RNIC registers to the SMR protocol, permission-switch latency can be reduced to the order of nanoseconds.

## 5 Evaluation

Our evaluation aims to answer the following:

- Q1 (Memory): How does mitigating memory accesses affect SafarDB’s performance?
- Q2 (Scaling): How does SafarDB (in FPGA-only mode) scale compared to existing systems?
- Q3 (Updates): How does SafarDB’s performance change with varying update percentages?
- Q4 (Fault): What are the effects of crash faults on SafarDB’s performance compared to existing systems?
- Q5 (Permission Switch): Does SafarDB benefit from an improved permission switch during crash-fault recovery?
- Q6 (Hybrid): What are the trade-offs of involving the host CPU in SafarDB’s hybrid mode?
- Q7 (Power): What are the power implications of SafarDB?

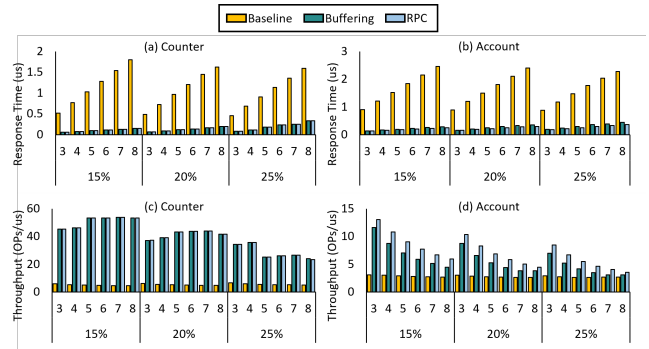


**Figure 6: Response time and throughput for one CRDT and one WRDT for three reducible transaction implementations.**

**Setup.** SafarDB was deployed on 8 AMD Xilinx Alveo U280s connected via 100GbE switches, with host Intel(R) Xeon(R) Gold 622R CPUs @ 2.90GHz at the Open Cloud Testbed (OCT) [95]. Each experiment runs for a total of 4 million operations, and depending on the experiment, with varying update percentages, node numbers, crash-faults, and workload distribution.

**Implementation.** We generate FPGA bitstreams for SafarDB usecases using Vivado 2023.2 and developed with Vitis HLS 2023.2, with intermediate IPs for the RDMA network stack using Vitis HLS 2020.2 and SystemVerilog. The RDMA stack is based off of StRoM [85]. The host CPU application is developed in C++ (version 11.4.0).

**Baselines.** We compare SafarDB against two equivalent systems:

- (1) Hamband [41]: Software RDT implementation utilizing Mu [3] for consensus; deployed on 8 Sapphire Rapids nodes at Texas A&M’s HPRC ACES cluster containing an Intel Xeon 8468 (Sapphire Rapids) CPU with 512 GB DDR5 memory, networked with an NVIDIA Mellanox NDR200 Infiniband RNIC (200Gbps) and connected by 400Gbps NDR400 InfiniBand network switches.
- (2) Waverunner [5]: Network-attached FPGA implementation of RAFT [70]; deployed on OCT with the same configuration as SafarDB, limited to 3 nodes due to Waverunner implementation.

**Workloads.** We have a micro benchmark that consists of a set of CRDTs (Table A.1)[83] and WRDTs (Table B.1)[40, 41] along with two widely used benchmarks: YCSB [32] and SmallBank [31].

CRDTs: (1) PN-Counter: A positive-negative counter that supports increment and decrement operations. A PN-Counter comprises two G-Counters: one for increments and one for decrements. (2) LWW-Register: A last-writer-wins register that supports assigning values to the register. Unique timestamps are associated with each assignment, ensuring a total order of operations. The register always retains the most recently written value. (3) G-Set: A grow-only set that supports addition, but not removal, of elements. (4) PN-Set: A set where a counter is associated with each element: addition increments the counter, and removal decrements the counter. An element is present if its counter is positive. (5) 2P-Set: A two-phase set that supports addition and removal of elements: once removed, an element cannot be reinserted into the set. A 2P-Set is typically implemented using two G-Sets.

WRDTs: (1) Account: A small-scale banking system which allows for depositing, withdrawing, and querying a single account. (2) Courseware: A school management system, which allows for

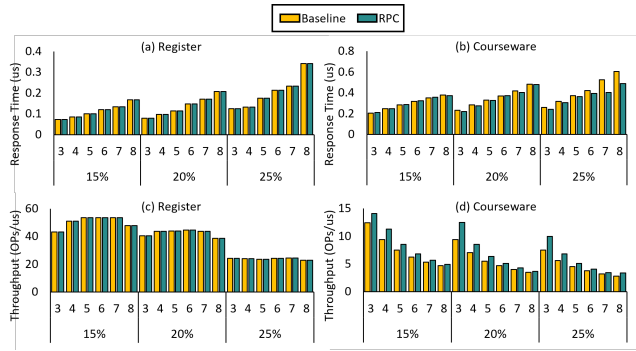


**Figure 7: Response time and throughput for one CRDT and one WRDT for two irreducible transactions**

courses and students to be added, and deleted, and students to enroll in courses. (3) Project: A project management system that allows for projects and employees to be added, deleted, and employees to be assigned to projects. (4) Movie: A movie theater ticketing systems that manages a set of customers and movies. (5) Auction: An online auctioning systems based on RUBis [25].

**Metrics.** We focus on three metrics: (1) *Response Time* ( $\mu\text{s}$ ): The average time from when a client issues an operation until it receives the corresponding response. (2) *Throughput* ( $\text{OPs}/\mu\text{s}$ ): The maximum number of operations per microsecond which the system completes. (3) *Power Consumption* ( $W$ ): FPGA power consumption is measured following AMD Xilinx Documentation [7]. CPU and I/O power consumption was measured with a combination of PowerTop [75] and Scaphandre [78].

## 5.1 Custom Verbs

To answer Q1, we conduct five experiments in which we measure the performance of SafarDB. In each experiment, we measure the response time and throughput of SafarDB when running CRDTs or WRDTs operations to see how memory accesses affect different transactions. The workloads are run for 4 million operations varying the number of nodes in the system and the percentage of operations that are updates versus reads. For example, in Figure 6a, the PN-Counter is run across 3-8 nodes for 15%, 20%, and 25% of the 4 million operations consisting of updates, while the remaining are query transactions, a read-only operation that retrieves the application state *e.g.*, returning the balance of a bank account.

The first pair of experiments (Figure 6) measures the impact of utilizing buffering and RDMA RPC to implement reducible transactions (subsection 4.1) on the PN-Counter and Account. For PN-counter, the buffered and RDMA RPC implementation exhibit 8 $\times$  lower response time and 7.8 $\times$  higher throughput than the baseline buffer-less design, due to each query and permissibility check not incurring a memory latency. The buffered implementation’s polling mechanism hides memory access latency from the applications critical path, and RDMA RPC eliminates them altogether. Buffering and RPC perform comparably for Counter (Figure 6a and c).

For Account, buffering and RDMA RPC reduces response time by 6.3 $\times$  and 7 $\times$ , while increasing response time 2 $\times$  and 2.4 $\times$ , respectively (Figure 6b and d). WRDT conflicting transactions require an SMR protocol (subsection 2.1), which designates one replica as a leader (subsection 4.4); the leader’s execution time is much greater than that of the followers. We observe that buffering cannot

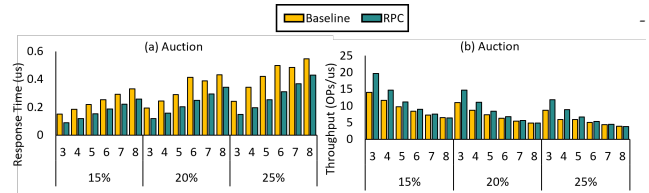


**Figure 8: Response time & throughput for one WRDT Auction (Table B.1) for two conflicting transaction implementations.**

fully hide memory accesses at the leader; but, RDMA RPC eliminates them and reduces execution time. For WRDTs, throughput depends on the leader’s execution time (noticeable impact), whereas response time is averaged across all replicas (marginal impact).

The second pair of experiments (Figure 7) measures the impact of utilizing RDMA RPC to implement irreducible transactions on the LWW-Register and Courseware. The results are similar to Figure 6. For the LWW register, all the memory accesses to the in-memory queues are hidden in the background, eliminating any possible advantage for RDMA RPC; this occurs because all replicas in a CRDT are peers (Figure 7 a and c).

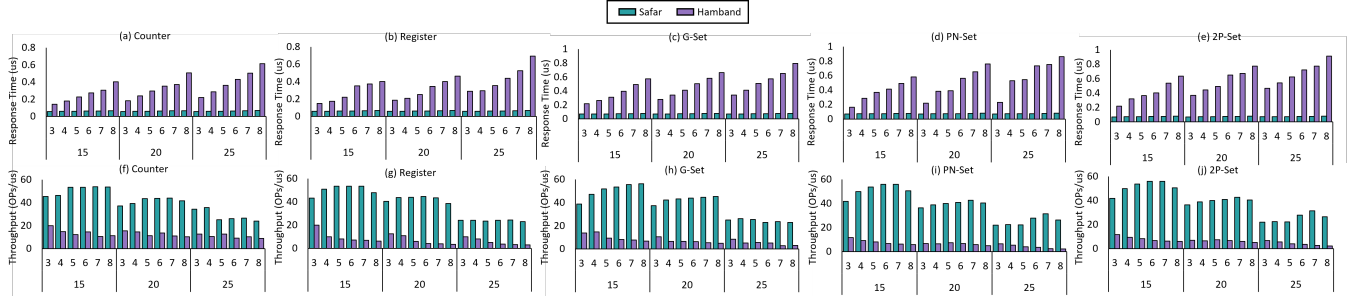
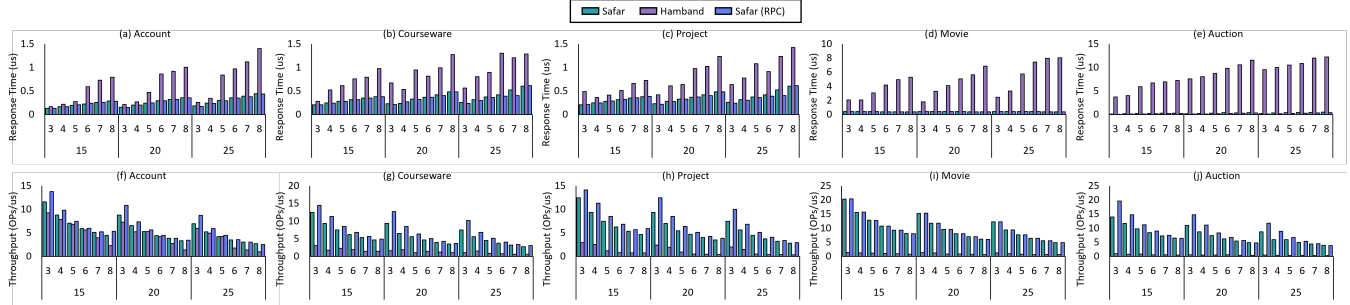
For Courseware, RPC achieves 1.04 $\times$  lower response times than the baseline, most visibly at 25% write percentage and 6–8 nodes. While RPC achieves 1.14 $\times$  higher throughput than the baseline, the advantage narrows as the number of replicas increases. These trends occur because conflicting transactions (described in the next section) access memory more often than non-conflicting transactions at the leader, so the baseline has fewer opportunities to hide memory access latencies. With a fixed number of transactions to execute, each replica executes fewer transactions as the number of replicas increases, thereby suppressing RDMA RPC’s throughput advantage at higher node counts.

The final experiment (Figure 8) measures the performance impact of utilizing RDMA RPC Write-Through for conflicting transactions. When implemented with RDMA write, conflicting transactions must access memory for *query* transactions and permissibility checks before executing. Auction exacerbates these accesses because it has three synchronization groups and three replication logs (one per group). RDMA RPC Write-Through updates the WRDT state immediately, ensuring it is up to date before subsequent *query* transactions and permissibility checks, removing the need for them to access the log. RDMA RPC Write-Through on average lowers response time by 1.5 $\times$  and raises throughput by 1.1 $\times$  across all write percentages and numbers of nodes in the networks, but only achieves higher throughput at low node counts. At lower node counts, followers benefit from fewer memory accesses, but at higher node counts, coordination (see subsection 4.4) emerges at the bottleneck, eliminating the advantage over RDMA write. These experiments answer Q1 by showing that adding buffer/polling or RDMA RPC to the implementation of the different transactions improve SafarDB’s overall performance.

## 5.2 Scalability

To answer Q2 and Q3, we conduct two sets of experiments, We evaluate SafarDB vs. Hamband, and SafarDB vs. Waverunner.

**SafarDB vs. Hamband.** Our first experiments compare SafarDB and Hamband on *five CRDT micro benchmarks*; each run executes one CRDT use case, as shown in Figure 9. SafarDB achieves 6 $\times$  lower response time and 6.2 $\times$  higher throughput in all instances. Increasing the number of replicas increasing response time by 2% and

Figure 9: Response Time ( $\mu\text{s}$ ) and Throughput (OPs/ $\mu\text{s}$ ) of CRDT use-casesFigure 10: Response Time ( $\mu\text{s}$ ) and Throughput (OPs/ $\mu\text{s}$ ) of WRDT use-cases

10% per replica for SafarDB and Hamband, respectively. SafarDB’s throughput actually increases by 2%, while Hamband’s decreases by 9.8% each replica. Increasing the update percentage increasing the response time by 1% and 36%, and decreases throughput by 50% and 43% for SafarDB and Hamband, respectively, when increasing from 15% to 25% update percentage. Increasing the number of replicas reduces the number of operations executed per replica, which benefits throughput. When increasing the number of replicas, we observe (1) increases in response time for both SafarDB and Hamband; (2) throughput increases for SafarDB; and (3) throughput is reduced for Hamband. We believe this is because Hamband must wait for completion queue ACKs before issuing the next RDMA verb or continuing with the application, as per the RDMA protocol spec, because our applications are inside an FPGA near data processing, and StRoM allows SafarDB to issue multiple RDMA verbs in sequence or interleave verbs with application logic, without waiting for ACKs. For CRDTs, SafarDB exhibits better scalability than Hamband.

Next five experiments comparing SafarDB and Hamband are *five WRDTs micro benchmarks*; each run executes one WRDT use case, as shown in Figure 10. Across all WRDTs, write percentages, and number of nodes in the network, SafarDB achieve 12 $\times$ , lower response time and 6.8 $\times$  higher throughput than Hamband. We believe that an important contributing factor is that the RDMA implementation on the network-attached FPGA eliminates sources of latency in a traditional CPU-based RDMA deployment (Figure 23a). Increasing the number of replicas increases response time by 7.3%, 8.8%, and 11.6% per replica for SafarDB, SafarDB (RPC), and Hamband, respectively; while decreasing throughput by 12%, 13.1% and 11.6% each replica. Increasing the update percentage increasing the response time by 26%, 17%, and 41%, and decreases throughput by 40%, 35% and 43% for SafarDB, SafarDB (RPC) and Hamband, respectively, when increasing from 15% to 25% update percentage.

SafarDB (RPC) achieves comparable response times to the baseline SafarDB for most of the experiments, with some advantages at higher write percentages and node counts (e.g., Courseware at 25% and 7-8 nodes). The one exception is Auction, where SafarDB (RPC) achieves lower response times than SafarDB (Baseline) across all runs, which we attribute to Auction having three synchronization groups, as well as two non-conflicting transactions. While Movie has two synchronization groups, it does not have a *query* transaction or non-conflicting transactions, which eliminates the situations where SafarDB (RPC) can reduce response time in comparison to SafarDB. Similarly, SafarDB (RPC) achieves higher throughput than SafarDB at lower node counts, with its advantage reduced at higher node counts in most experiments. The one exception is Movie, where SafarDB (RPC) and SafarDB achieve comparable throughput, for the same reasons.

Ultimately, we see that both SafarDB and SafarDB (RPC) clearly outperform Hamband; while the advantages of SafarDB (RPC) over SafarDB are somewhat limited, we see no instances in which SafarDB clearly outperforms SafarDB (RPC). For these reasons, we conclude that SafarDB (RPC) is a superior approach to implementing WRDTs for network-attached FPGAs; it can be used when system designers cannot to augment the RDMA stack with FPGA-specific verbs.

Our last two experiments comparing SafarDB and Hamband are for the YCSB and SmallBank workload (Figure 11). For both YCSB and SmallBank, SafarDB scales to 8 nodes, while Hamband does not, and SafarDB achieves, on average, 8 $\times$  lower response time and 5.2 $\times$  higher throughput, respectively. Hamband is able to outperform SafarDB on the read-only workload (0% update) due to the larger cache of Hamband’s baseline CPU fitting all the stores. The drastic drop in performance in SmallBank (Figure 11 c and d) from 0% update to 5% for both SafarDB and Hamband is attributed to the need for SMR in the SmallBank workload.

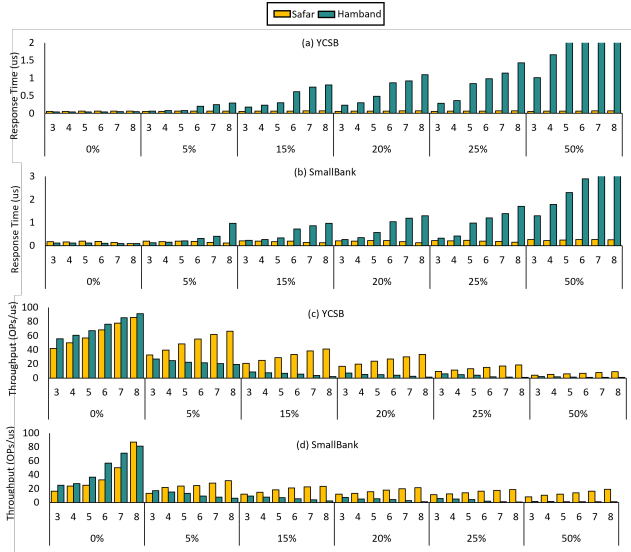


Figure 11: Response time & throughput: YCSB/SmallBank

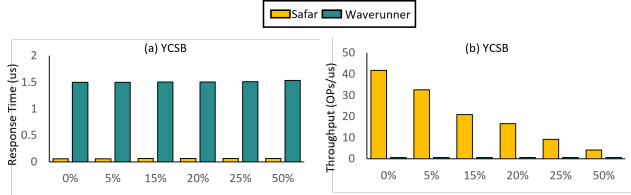


Figure 12: SafarDB vs. Waverunner response time and throughput on three nodes.

**SafarDB vs. Waverunner.** Last experiment, SafarDB is compared to Waverunner running YCSB on three nodes (Figure 12). We report results for different PUT/GET ratios. Waverunner is a state-of-the-art FPGA-based SmartNIC system that accelerates the consensus/SMR replication path in distributed systems [5]. They implement an accelerated Raft setup with three replicas (one leader and two followers). The leader is responsible for handling client requests (in the fast path these requests are processed as packets), while followers do not serve client requests directly. SafarDB provides 25.5 $\times$  lower response time and 31.3 $\times$  higher throughput. Main reason is that in SafarDB, the application is implemented inside the FPGA, so near-data processing reduces response time. In Waverunner, the application runs in software on the hosts, and the FPGA mainly accelerates replication. Due to hybrid consistency, SafarDB can handle client requests on all nodes, while in Waverunner, only the leader handles client requests; if a client contacts a follower, the follower rejects it, and the client must resend to the leader.

These experiments answer Q2 by showing that SafarDB is able to out scale Hamband across multiple different applications, and perform better than Waverunner in YCSB. SafarDB is also shown to scale as the update % increases answering Q3.

### 5.3 Fault Tolerance

To answer Q4 and Q5, we evaluate (1) the latency/variability of permission switches, and (2) the impact of single-node crash failures on both CRDT and WRDT executions. Figure 13 compares

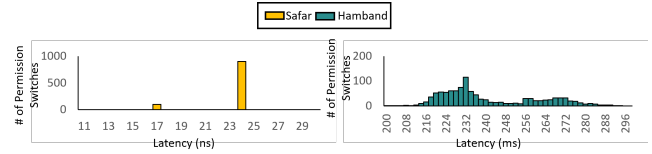


Figure 13: Permission Switch histograms

the round-trip time of changing write permissions in SafarDB’s networked-attached FPGA implementation and Hamband’s traditional RDMA network [3, 41]. The latter incurs overhead accruing to PCIe traffic, thread-switching, and RNIC caching, leading to high variability in round-trip time. In contrast, SafarDB’s direct connection within the FPGA between the WRDT user kernel accelerator and Network kernel exhibits greater stability: either 17 or 24 ns, and orders of magnitude faster than a traditional RDMA network. The impact of this reduced permission switch latency on failure recovery is elucidated in Figure 14. This directly benefits crash-fault recovery for WRDTs: after a leader failure, recovery requires revoking and re-granting write permissions at the newly elected leader, and SafarDB’s low and stable permission-switch latency reduces the recovery overhead on the critical path.

This subsection evaluates the impact of crash-failures on one CRDT (2PSet) and one WRDT (Bank Account). Experiments are performed with four nodes and varying write percentages. We simulate crash failures by stopping a preselected node during execution; the remaining operations are redistributed to the other replicas.

**Replica Failure:** In Figure 14e and 14f, the failure of one 2P-Set replica decreases SafarDB’s response time by 2% and Hamband’s by 8%, and reduces SafarDB’s throughput by 12% and Hamband’s by 9%. After the failure, the response time for both SafarDB and Hamband goes down because there is one less remote node to replicate to, which reduces replication time. However, throughput goes down as well because the failure reduces the level of parallelism: with one less node, there is one less replica to handle requests. Even in the presence of a node failure, SafarDB outperforms Hamband by both measures, indicating that single-node failures do not compromise the benefits of FPGA acceleration.

**Follower Failure:** In Figure 14 a and b, failure of one Account’s follower has no visible impact on SafarDB’s response time while increasing Hamband’s by 1.4 $\times$ , while reducing SafarDB’s throughput by around 2% and Hamband’s by 30%. SafarDB’s response time is not impacted as the other followers can immediately start executing the redistributed operations without waiting; throughput minimally decreases due to the need to update the leader’s follower list to remove the failed node by monitoring heartbeats.

For WRDTs, stopping any replica prevents its heartbeat from incrementing. The leader maintains a list of known followers; when the leader detects that a follower fails, it removes the failed follower from its list. In Hamband, this update occurs in the foreground and impacts leader execution time; SafarDB updates the follower list in the background, which mostly hides the latency.

**Leader Failure:** In Figure 14 c and d, failure of Account’s leader triggers a new leader election, with operations redistributed *after* the election to the newly elected leader and two remaining followers. SafarDB’s response time increases by around 25%, and Hamband’s by around 40%; SafarDB’s throughput is reduced by a modest 15%, and Hamband’s by a more significant 40%. SafarDB benefits from the

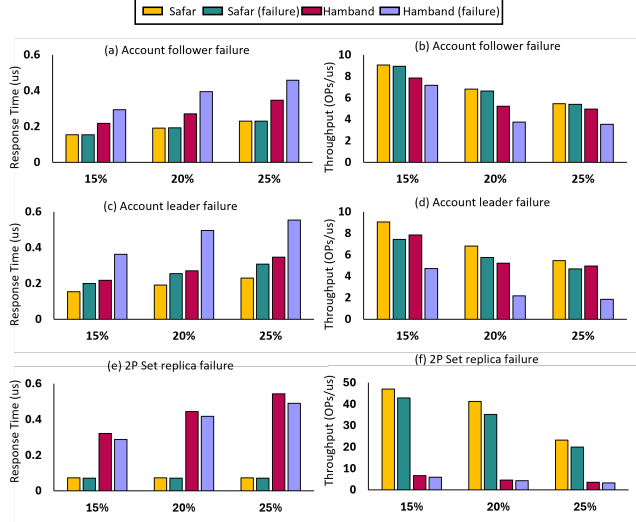


Figure 14: Fault Tolerance experiments

faster permission switch (Figure 13). At a write percentage of 15%, SafarDB’s throughput in the presence of leader failure is reduced beneath that of Hamband running without failure; this is due to the performance impact of leader elections, which do incur network latencies that cannot be fully hidden; at higher write percentages, SafarDB’s throughput when the leader failures remains higher than Hamband’s throughput without failure.

These experiments answer Q4 by showing that crash faults can reduce throughput due to reduced parallelism and (for leader failures) leader-election overheads, while response time can decrease for CRDTs because there is one less remote replica to update. They also answer Q5 by showing that SafarDB’s fast and stable permission switch reduces the recovery overhead in leader-failure, contributing to lower recovery cost than traditional RDMA deployments.

## 5.4 Hybrid

To answer Q6, we evaluate the trade-offs of involving the host CPU in SafarDB’s hybrid mode using YCSB and SmallBank. We conduct three experiments: (1) varying the percentage of operations that target FPGA-resident data (Operations Assignment), (2) studying access skew under Zipfian workloads (Workload Distribution), and (3) applying summarization to batch remote updates (Summarization).

**Operations Assignment.** With our first set of experiments (Figure 15), we study SafarDB’s flexibility and address the practical concern: when the whole application does not fit inside the FPGA. In hybrid mode, we implement part of YCSB and SmallBank on the host and part inside the FPGA. For YCSB 100K, keys are stored inside the FPGA, and the remaining 10M keys are in CPU host memory. As for SmallBank, 10M accounts are within the FPGA, and the remaining 90M accounts are stored within CPU host memory. We then vary the fraction of the workload assigned to the FPGA versus the host—meaning we change the rate of client requests that target FPGA-resident keys/accounts versus the host-resident keys/accounts, and we report response time and throughput.

As larger portions of operations are served by the FPGA, response time decreases and throughput increases approximately linearly as less PCIe communication occurs during execution (e.g.,

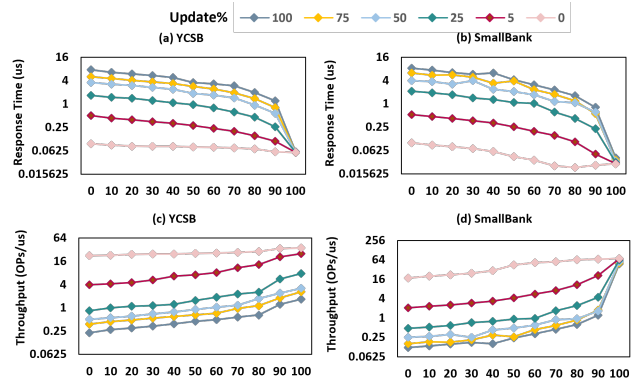


Figure 15: Response time and throughput for YCSB/SmallBank with different percentages of OPs assigned to the FPGA.

in YCSB at 50% writes, response time decreases by 5.7 $\times$  and throughput increases by 4.7 $\times$  when we increase the fraction of operations assigned to the FPGA from 10% to 90%). By invoking the hybrid mode for these workloads, a small hit in performance is compensated for with an increase in application size while still delivering good response time and throughput for microsecond applications. This highlights a core trade-off in hybrid mode: host memory expands capacity beyond the FPGA, but performance improves as more requests are served by FPGA-resident hot keys/accounts.

**Workload Distribution.** Our second set of hybrid experiments (Figure 16) studies the effects of workload (uniform vs. Zipfian) distributions on SafarDB’s hybrid mode. We present the effect of skew on three different update ratios, 0%, 5%, and 50%, on different hybrid configurations. In YCSB, the distribution is across the different keys, while SmallBank is across the different accounts. A  $\theta = 0$  value is a uniform distribution, with 2 representing a high skew Zipfian distribution, e.g., in Smallbank with a  $\theta = 2$  would represent a small subset of hot bank accounts.

Increasing the skew shows its effect when we have a higher fraction of reads, and when more requests target host-resident keys. For example, in YCSB at 0% writes, when 20% of operations are assigned to the FPGA, increasing the skewness from 0 to 1.2 decreases response time by 2.5 $\times$  and increases throughput by 2.3 $\times$ ; however, with the same write ratio, when 80% of operations are assigned to the FPGA, we observe a 1.5 $\times$  decrease in response time and a 1.5 $\times$  increase in throughput. The reason is cache locality: with higher skew, the hot host keys are reused more and stay in the CPU caches, so host-side accesses become faster. Because of this, increasing skewness has little effect on the response time or throughput of (1) read operations that hit FPGA-resident keys, and (2) read/write operations where the key is inside the FPGA-resident set. Therefore, when the write ratio is higher, or when a larger fraction of requests are to FPGA-resident keys, the improvement from skew in response time and throughput becomes minimal. For example, in YCSB at 50% writes, when 20% of operations are assigned to the FPGA, increasing the skewness from 0 to 1.2 decreases response time by 1.3 $\times$  and increases throughput by 1.2 $\times$ . Thus, SafarDB’s hybrid mode exposes a second trade-off: skew can partially compensate

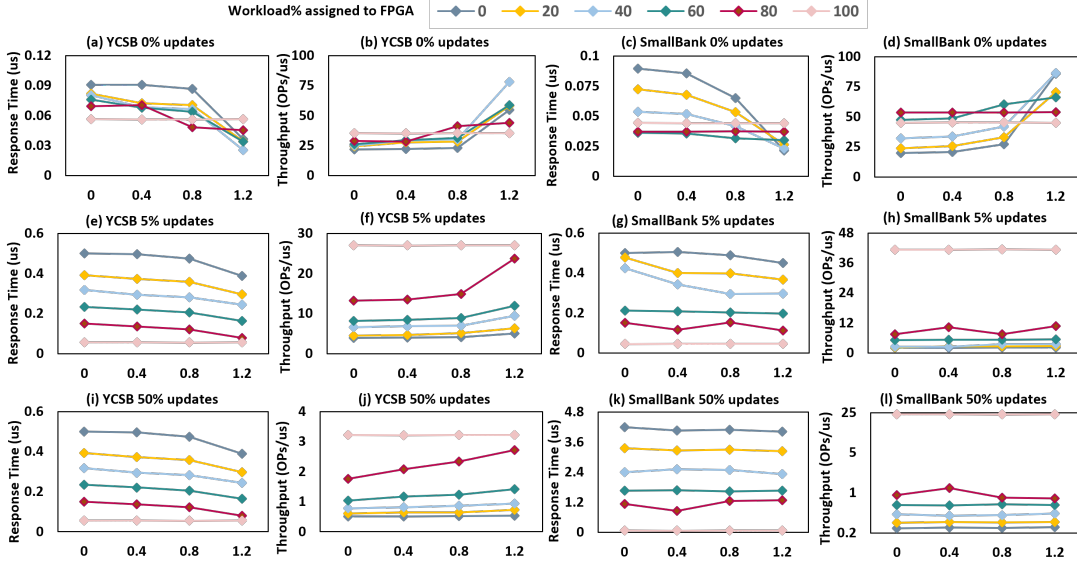


Figure 16: Response time and throughput for YCSB and SmallBank with different  $\theta$  values of Zipfian.

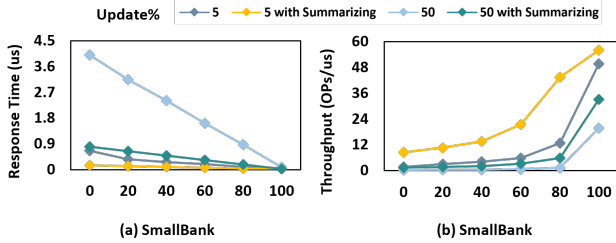


Figure 17: Response time and throughput for SmallBank with a summarization size of 5 in different hybrid percentages.

for host accesses via CPU caching, but this benefit diminishes as writes increase or as more requests are served inside the FPGA.

**Summarization.** Our experiment studies the effect of summarization on SafarDB’s response time and throughput when we vary the percentage of operations assigned to the FPGA while running the SmallBank application. With summarization, instead of updating the remote replicas via RDMA or coordination after receiving client requests, we only update the local state, and whenever we reach the summarization threshold, we propagate the updates to the remote replicas. This helps avoid the cost of updating remote replicas for every transaction, since we update them only after processing a batch of transactions determined by the summarization size (in this experiment, the summarization size is 5). Figure 17 shows the effect of summarization. As seen, response time decreases and throughput increases as the summarization size increases; for example, in SmallBank under a write-heavy workload (50% write), when 40% of operations are assigned to the FPGA, summarization decreases response time by 4.9 $\times$  and increases throughput by 5 $\times$ . This improves system performance, but it also increases staleness. Therefore, summarization introduces a third trade-off in hybrid mode: batching improves response time and throughput by reducing per-operation replication overhead, at the cost of higher staleness between synchronizations.

These experiments answer Q6 by showing that SafarDB’s hybrid mode enables scaling to larger datasets by placing cold keys on the host while keeping hot keys on the FPGA; performance improves as more operations hit FPGA-resident data, host-side skew can

mitigate CPU accesses via caching, and summarization improves performance by batching updates at the cost of increased staleness.

## 5.5 Power

SafarDB consumes about 35W, while Hamband consumes about 160W; SafarDB consumes approximately 4.5 $\times$  less power than Hamband (Figure is in the appendix.). The power consumption reported for SafarDB includes both the FPGA and HBM. For Hamband, approximately two-thirds of the power consumption is due to the CPU, and one-third is due to I/O, which includes memory, the RDMA NIC, the PCIe interface, etc. FPGAs consume less power than CPUs for many reasons. For example, they operate at lower clock frequencies, do not incur data-movement overheads comparable to those of a cache hierarchy, and do not run an operating system [51].

## 6 Related Work

To the best of our knowledge, SafarDB represents the first attempt to accelerate RDTs using FPGAs. We first discuss work on consensus/SMR and FPGA acceleration of replication control paths, which relates to SafarDB’s support for strongly ordered operations. SMR protocols, which are needed for WRDT conflicting transactions, have been designed for message-passing [27, 42, 54, 67, 69, 71] and RDMA [3, 4, 36, 45, 47, 48, 66, 74, 87, 89, 94] networks. In terms of hardware acceleration, HovercRaft [50] and Waverunner [5] accelerate Raft [71] using an in-network programmable P4 ASIC and an FPGA-based Soft NIC, respectively. Consensus-in-a-Box (CBox) [44] implements the full Zookeeper Atomic Broadcast (ZAB) protocol [42, 67], including leader election, failure recovery, and application code on the FPGA while storing the replication log in onboard DRAM. We opted to implement Mu [3] on the FPGA as our RDT implementations were RDMA-based; non-RDMA-based RDTs could be ported to network-attached FPGAs using either Waverunner or CBox to provide consensus.

Next, we review RDMA/RPC communication primitives and NIC mechanisms that reduce host overheads, which SafarDB builds upon and extends for FPGA-resident execution. SafarDB relates to prior proposals for new RDMA verbs. For example, Prism [22] introduces

new primitives to support common remote access patterns, StRoM [85] and RMC [8] propose new RDMA verbs to support remote procedure calls (RPCs), and KV-direct [58] evaluates four RDMA verbs that accelerate key-value stores. The nanoPu provides an RDMA-inspired fast path between the NIC and CPU register file to support  $\mu$ s-scale RPCs [43]. Either Hamband’s or SafarDB’s RDTs may further benefit from Prism’s primitives or nanoPU acceleration. SafarDB’s SMR, coupled with KV-direct’s custom RDMA verbs, could accelerate a replicated key-value store.

Finally, we summarize SmartNIC and programmable-NIC designs, and clarify how SafarDB differs by integrating the NIC and replication engine on a network-attached FPGA. Smart NICs [24, 33–35, 76] integrate programmable accelerators, allowing servers to offload tasks relating to networking to the network interface. *On-path* (“bump in the wire”) Smart NICs place programmable elements on the packet processing path, which adds latency when they are not utilized, while *Off-path* Smart NICs [65, 80, 91] integrate a network switch, which removes the programmable elements from the packet processing path, but adds a small amount of routing latency. Prior work has noted a lack of versatility in Smart NIC functionality, as Smart NICs are often limited to specific tasks such as RDMA [39]. Unlike Smart NICs, SafarDB’s network stack is implemented within the FPGA; while less efficient than using an ASIC, SafarDB eliminates inter-chip communication overheads which are inherent to Smart NICs, while enabling application developers design and deploy application or domain-specific on-path, off-path, or hybrid communication architectures.

## 7 Conclusion

SafarDB demonstrates that replicated data types can be efficiently implemented directly on network-attached FPGAs, significantly outperforming state-of-the-art RDMA-based and FPGA-accelerated designs. These gains stem from tightly integrating RDT accelerators with an RDMA-capable NIC on a single FPGA, enabling low-latency communication among FPGA-resident components, direct access to on-chip storage, and specialized RDMA verbs that eliminate software and host CPU overheads. Importantly, experiments show that these benefits extend beyond microbenchmarks to replicated transactional workloads and database replication (e.g., YCSB and SmallBank). Together, these results suggest that co-designing NICs and consistency primitives on programmable network-attached hardware is a promising direction for building low-latency, high-throughput replicated transactional systems and database replication.

## References

- [1] 2016. Memcached. <http://memcached.org/>.
- [2] Daniel Abadi. 2012. Consistency Tradeoffs in Modern Distributed Database System Design. *Computer* 45, 2 (2012), 6 pages.
- [3] Marcos K. Aguilera, Naama Ben-David, Rachid Guerraoui, Virendra J. Marathe, Athanasios Xygkis, and Igor Zablotchi. 2020. Microsecond Consensus for Microsecond Applications. In *Proceedings of the 14th USENIX Conference on Operating Systems Design and Implementation (OSDI’20)*. USENIX Association, USA, Article 34, 18 pages.
- [4] Marcos K. Aguilera, Naama Ben-David, Rachid Guerraoui, Antoine Murat, Athanasios Xygkis, and Igor Zablotchi. 2023. uBFT: Microsecond-Scale BFT using Disaggregated Memory. In *Proceedings of the 28th ACM International Conference on Architectural Support for Programming Languages and Operating Systems, Volume 2, ASPLOS 2023, Vancouver, BC, Canada, March 25–29, 2023*, Tor M.

- Aamodt, Natalie D. Enright Jerger, and Michael M. Swift (Eds.). ACM, 862–877. doi:10.1145/3575693.3575732
- [5] Mohammadreza Alimadadi, Hieu Mai, Shenghsun Cho, Michael Ferdman, Peter A. Milder, and Shuai Mu. 2023. Waverunner: An Elegant Approach to Hardware Acceleration of State Machine Replication. In *20th USENIX Symposium on Networked Systems Design and Implementation, NSDI 2023, Boston, MA, April 17–19, 2023*, Mahesh Balakrishnan and Manya Ghobadi (Eds.). USENIX Association, 357–374. <https://www.usenix.org/conference/nsdi23/presentation/alimadadi>
- [6] Paulo Sérgio Almeida, Ali Shoker, and Carlos Baquero. 2015. Efficient State-Based CRDTs by Delta-Mutation. In *Networked Systems - Third International Conference, NETYS 2015, Agadir, Morocco, May 13–15, 2015, Revised Selected Papers (Lecture Notes in Computer Science, Vol. 9466)*, Ahmed Bouajjani and Hugues Fauconnier (Eds.). Springer, 62–76. doi:10.1007/978-3-319-26850-7\_5
- [7] Alveo Card Management Solution Subsystem Product Guide 2023. <https://docs.amveo.com/r/en-US/pg348-cms-subsystem/Sensor-Monitoring>.
- [8] Emmanuel Amaro, Zhihong Luo, Amy Ousterhout, Arvind Krishnamurthy, Aurajit Panda, Sylvia Ratnasamy, and Scott Shenker. 2020. Remote Memory Calls. In *HotNets ’20: The 19th ACM Workshop on Hot Topics in Networks, Virtual Event, USA, November 4–6, 2020*, Ben Y. Zhao, Heather Zheng, Harsha V. Madhyastha, and Venkat N. Padmanabhan (Eds.). ACM, 38–44. doi:10.1145/3422604.3425923
- [9] Wei Bai, Shanin Sainul Abdeen, Ankit Agrawal, Krishan Kumar Attre, Paramvir Bahl, Ameya Bhagat, Gowri Bhaskara, Tanya Brokhaman, Lei Cao, Ahmad Cheema, Rebecca Chow, Jeff Cohen, Mahmoud Elhaddad, Vivek Ette, Igal Figlin, Daniel Firestone, Mathew George, Ilya German, Lakhmeet Ghai, Eric Green, Albert G. Greenberg, Manish Gupta, Randy Haagens, Matthew Hendel, Ridwan Howlader, Neetha John, Julia Johnstone, Tom Jolly, Greg Kramer, David Kruse, Ankit Kumar, Erica Lan, Ivan Lee, Avi Levy, Marina Lipshteyn, Xin Liu, Chen Liu, Guohan Lu, Yuemin Lu, Xiakun Lu, Vadim Makhervaks, Ulad Malashanka, David A. Maltz, Ilias Marinou, Rohan Mehta, Sharda Murthi, Anup Namdhari, Aaron Ogun, Jitendra Padhye, Madhav Pandya, Douglas Phillips, Adrian Power, Suraj Puri, Shachar Raindel, Jordan Rhee, Anthony Russo, Maneesh Sah, Ali Sherif, Chris Sparacino, Ashutosh Srivastava, Weixiang Sun, Nick Swanson, Fuhou Tian, Lukasz Tomczyk, Vamsi Vadlamuri, Alec Wolman, Ying Xie, Joyce Yom, Lihua Yuan, Yanzhao Zhang, and Brian Zill. 2023. Empowering Azure Storage with RDMA. In *20th USENIX Symposium on Networked Systems Design and Implementation, NSDI 2023, Boston, MA, April 17–19, 2023*, Mahesh Balakrishnan and Manya Ghobadi (Eds.). USENIX Association, 49–67. <https://www.usenix.org/conference/nsdi23/presentation/bai>
- [10] Peter Bailis, Alan Fekete, Michael J. Franklin, Ali Ghodsi, Joseph M. Hellerstein, and Ion Stoica. 2014. Coordination Avoidance in Database Systems. *Proc. VLDB Endow.* 8, 3 (Nov. 2014), 185–196.
- [11] Peter Bailis, Alan Fekete, Michael J. Franklin, Ali Ghodsi, Joseph M. Hellerstein, and Ion Stoica. 2015. Feral concurrency control: An empirical investigation of modern application integrity. In *Proceedings of the 2015 ACM SIGMOD International Conference on Management of Data*. 1327–1342.
- [12] Valter Balegas, Sérgio Duarte, Carla Ferreira, Rodrigo Rodrigues, and Nuno Preguica. 2012. IPA: Invariant-Preserving Applications for Weakly Consistent Replicated Databases. *Proceedings of the VLDB Endowment* 12, 4 (2012).
- [13] Valter Balegas, Sérgio Duarte, Carla Ferreira, Rodrigo Rodrigues, Nuno Preguica, Mahsa Najafzadeh, and Marc Shapiro. 2015. Putting Consistency Back into Eventual Consistency. In *Proceedings of the Tenth European Conference on Computer Systems (Bordeaux, France) (EuroSys ’15)*. ACM, New York, NY, USA, Article 6, 16 pages.
- [14] Valter Balegas, Sérgio Duarte, Carla Ferreira, Rodrigo Rodrigues, Nuno Preguica, Mahsa Najafzadeh, and Marc Shapiro. 2015. Towards Fast Invariant Preservation in Geo-replicated Systems. *SIGOPS Oper. Syst. Rev.* 49, 1 (Jan. 2015), 121–125. doi:10.1145/2723872.2723889
- [15] Carlos Baquero, Paulo Sérgio Almeida, and Ali Shoker. 2014. Making Operation-Based CRDTs Operation-Based. In *Distributed Applications and Interoperable Systems - 14th IFIP WG 6.1 International Conference, DAIS 2014, Held as Part of the 9th International Federated Conference on Distributed Computing Techniques, DisCoTec 2014, Berlin, Germany, June 3–5, 2014, Proceedings (Lecture Notes in Computer Science, Vol. 8460)*, Kostas Magoutis and Peter R. Pietzuch (Eds.). Springer, 126–140. doi:10.1007/978-3-662-43352-2\_11
- [16] Carlos Baquero and Francisco Moura. 1999. Using Structural Characteristics for Autonomous Operation. *ACM SIGOPS Oper. Syst. Rev.* 33, 4 (1999), 90–96. doi:10.1145/334598.334614
- [17] Luiz André Barroso, Mike Marty, David A. Patterson, and Parthasarathy Ranganathan. 2017. Attack of the killer microseconds. *Commun. ACM* 60, 4 (2017), 48–54. doi:10.1145/3015146
- [18] Carsten Binnig and Nesime Tatbul. 2024. International Workshop on Data Management on New Hardware (DaMoN). In *Companion of the 2024 International Conference on Management of Data (Santiago AA, Chile) (SIGMOD ’24)*. Association for Computing Machinery, New York, NY, USA, 645–646. doi:10.1145/3626246.3655011
- [19] Eric Brewer. 2012. CAP twelve years later: How the “rules” have changed. *Computer* 45, 2 (2012), 23–29.

- [20] Eric A Brewer. 2000. Towards robust distributed systems. In *PODC*, Vol. 7. Portland, OR, 343477–343502.
- [21] Sebastian Burckhardt, Alexey Gotsman, Hongseok Yang, and Marek Zawirski. 2014. Replicated data types: specification, verification, optimality. In *The 41st Annual ACM SIGPLAN-SIGACT Symposium on Principles of Programming Languages, POPL '14, San Diego, CA, USA, January 20–21, 2014*, Suresh Jagannathan and Peter Sewell (Eds.). ACM, 271–284. doi:10.1145/2535838.2535848
- [22] Matthew Burke, Sowmya Dharanipragada, Shannon Joyner, Adriana Szekeres, Jacob Nelson, Irene Zhang, and Dan R. K. Ports. 2021. PRISM: Rethinking the RDMA Interface for Distributed Systems. In *Proceedings of the ACM SIGOPS 28th Symposium on Operating Systems Principles (Virtual Event, Germany) (SOSP '21)*. Association for Computing Machinery, New York, NY, USA, 228–242. doi:10.1145/3477132.3483587
- [23] Mike Burrows. 2006. The Chubby Lock Service for Loosely-coupled Distributed Systems. In *Proceedings of the 7th Symposium on Operating Systems Design and Implementation (Seattle, Washington) (OSDI '06)*. USENIX Association, Berkeley, CA, USA, 335–350.
- [24] Adrian M. Caulfield, Eric S. Chung, Andrew Putnam, Hari Angepat, Jeremy Fowers, Michael Haselman, Stephen Heil, Matt Humphrey, Puneet Kaur, Joo-Young Kim, Daniel Lo, Todd Massengill, Kalin Ovtcharov, Michael Papatimichael, Lisa Woods, Sitaram Lanka, Derek Chiou, and Doug Burger. 2016. A cloud-scale acceleration architecture. In *49th Annual IEEE/ACM International Symposium on Microarchitecture, MICRO 2016, Taipei, Taiwan, October 15–19, 2016*. IEEE Computer Society, 7:1–7:13. doi:10.1109/MICRO.2016.7783710
- [25] Emmanuel Cecchet and Julie Marguerite. 2009. Rubis: Rice university bidding system.
- [26] Brian F Cooper, Raghu Ramakrishnan, Utkarsh Srivastava, Adam Silberstein, Philip Bohannon, Hans-Arno Jacobsen, Nick Puz, Daniel Weaver, and Ramana Yerneni. 2008. Pnuts: Yahoo!'s hosted data serving platform. *Proceedings of the VLDB Endowment* 1, 2 (2008), 1277–1288.
- [27] James C. Corbett, Jeffrey Dean, Michael Epstein, Andrew Fikes, Christopher Frost, J. J. Furman, Sanjay Ghemawat, Andrey Gubarev, Christopher Heiser, Peter Hochschild, Wilson Hsieh, Sebastian Kanthak, Eugene Kogan, Hongyi Li, Alexander Lloyd, Sergey Melnik, David Mwaura, David Nagle, Sean Quinlan, Rajesh Rao, Lindsay Rolig, Yasushi Saito, Michal Szymaniak, Christopher Taylor, Ruth Wang, and Dale Woodford. 2013. Spanner: Google's Globally Distributed Database. *ACM Trans. Comput. Syst.* 31, 3, Article 8 (Aug. 2013), 22 pages.
- [28] William J. Dally, James D. Balfour, David Black-Schaffer, James Chen, R. Curtis Harting, Vishal Parikh, JongSoo Park, and David Sheffield. 2008. Efficient Embedded Computing. *Computer* 41, 7 (2008), 27–32. doi:10.1109/MC.2008.224
- [29] Kevin De Porre, Carla Ferreira, Nuno Pregoica, and Elisa Gonzalez Boix. 2021. ECROS: building global scale systems from sequential code. *Proceedings of the ACM on Programming Languages* 5, OOPSLA (2021), 1–30.
- [30] Giuseppe DeCandia, Deniz Hastorun, Madan Jampani, Gunavardhan Kakulapati, Avinash Lakshman, Alex Pilchin, Swaminathan Sivasubramanian, Peter Vosshall, and Werner Vogels. 2007. Dynamo: amazon's highly available key-value store. In *Proceedings of the 21st ACM Symposium on Operating Systems Principles 2007, SOSP 2007, Stevenson, Washington, USA, October 14–17, 2007*, Thomas C. Bressoud and M. Frans Kaashoek (Eds.). ACM, 205–220. doi:10.1145/1294261.1294281
- [31] Djelle Eddine Difallah, Andrew Pavlo, Carlo Curino, and Philippe Cudre-Mauroux. 2013. OLTP-Bench: an extensible testbed for benchmarking relational databases. *Proc. VLDB Endow.* 7, 4 (Dec. 2013), 277–288. doi:10.14778/2732240.2732246
- [32] Tien Tuan Anh Dinh, Ji Wang, Gang Chen, Rui Liu, Beng Chin Ooi, and Kian-Lee Tan. 2017. BLOCKBENCH: A Framework for Analyzing Private Blockchains. In *Proceedings of the 2017 ACM International Conference on Management of Data (Chicago, Illinois, USA) (SIGMOD '17)*. Association for Computing Machinery, New York, NY, USA, 1085–1100. doi:10.1145/3035918.3064033
- [33] Daniel Firestone. 2017. VFP: A Virtual Switch Platform for Host SDN in the Public Cloud. In *14th USENIX Symposium on Networked Systems Design and Implementation, NSDI 2017, Boston, MA, USA, March 27–29, 2017*, Aditya Akella and Jon Howell (Eds.). USENIX Association, 315–328. <https://www.usenix.org/conference/nsdi17/technical-sessions/presentation/firestone>
- [34] Daniel Firestone, Andrew Putnam, Sambrama Mundkur, Derek Chiou, Alireza Dabagh, Mike Andrewartha, Hari Angepat, Vivek Bhanu, Adrian M. Caulfield, Eric S. Chung, Harish Kumar Chandrappa, Somesh Chaturmohita, Matt Humphrey, Jack Lavier, Norman Lam, Fengfen Liu, Kalin Ovtcharov, Jitu Padhye, Gautham Popuri, Shachar Raindel, Tejas Sapre, Mark Shaw, Gabriel Silva, Madhan Sivakumar, Nisheeth Srivastava, Anshuman Verma, Qasim Zuhair, Deepak Bansal, Doug Burger, Kushagra Vaid, David A. Maltz, and Albert G. Greenberg. 2018. Azure Accelerated Networking: SmartNICs in the Public Cloud. In *15th USENIX Symposium on Networked Systems Design and Implementation, NSDI 2018, Renton, WA, USA, April 9–11, 2018*, Sujata Banerjee and Srinivasan Seshan (Eds.). USENIX Association, 51–66. <https://www.usenix.org/conference/nsdi18/presentation/firestone>
- [35] Jeremy Fowers, Kalin Ovtcharov, Michael Papatimichael, Todd Massengill, Ming Liu, Daniel Lo, Shlomi Alkalay, Michael Haselman, Logan Adams, Mahdi Ghandi, Stephen Heil, Prerak Patel, Adam Sapek, Gabriel Weisz, Lisa Woods, Sitaram Lanka, Steven K. Reinhardt, Adrian M. Caulfield, Eric S. Chung, and Doug Burger. 2018. A Configurable Cloud-Scale DNN Processor for Real-Time AI. In *45th Annual International Symposium on Computer Architecture, ISCA 2018, Los Angeles, CA, USA, June 1–6, 2018*, Murali Annamaram, Timothy Mark Pinkston, and Babak Falsafi (Eds.). IEEE Computer Society, 1–14. doi:10.1109/ISCA.2018.00012
- [36] Vasilis Gavrielatos, Antonios Katsarakis, and Vijay Nagarajan. 2021. Odyssey: the impact of modern hardware on strongly-consistent replication protocols. In *EuroSys '21: Sixteenth European Conference on Computer Systems, Online Event, United Kingdom, April 26–28, 2021*, Antonio Barbalace, Pramod Bhatotia, Lorenzo Alvisi, and Cristian Cadar (Eds.). ACM, 245–260. doi:10.1145/3447786.3456240
- [37] Alexey Gotsman, Hongseok Yang, Carla Ferreira, Mahsa Najafzadeh, and Marc Shapiro. 2016. 'Cause I'M Strong Enough: Reasoning About Consistency Choices in Distributed Systems. In *Proceedings of the 43rd Annual ACM SIGPLAN-SIGACT Symposium on Principles of Programming Languages (St. Petersburg, FL, USA) (POPL '16)*. ACM, New York, NY, USA, 371–384. doi:10.1145/2837614.2837625
- [38] Rehan Hameed, Wajahat Qadeer, Megan Wachs, Komiz Azizi, Alex Solomatnikov, Benjamin C. Lee, Stephen Richardson, Christos Kozyrakis, and Mark Horowitz. 2010. Understanding sources of inefficiency in general-purpose chips. In *37th International Symposium on Computer Architecture (ISCA 2010), June 19–23, 2010, Saint-Malo, France*, André Seznec, Uri C. Weiser, and Ronny Ronen (Eds.). ACM, 37–47. doi:10.1145/1815961.1815968
- [39] Torsten Hoefler, Salvatore Di Girolamo, Konstantin Taranov, Ryan E. Grant, and Ron Brightwell. 2017. SPIN: High-Performance Streaming Processing In the Network. In *Proceedings of the International Conference for High Performance Computing, Networking, Storage and Analysis (Denver, Colorado) (SC '17)*. Association for Computing Machinery, New York, NY, USA, Article 59, 16 pages. doi:10.1145/3126908.3126970
- [40] Farzin Houshmand and Mohsen Lesani. 2019. Hamsaz: replication coordination analysis and synthesis. *Proc. ACM Program. Lang.* 3, POPL (2019), 74:1–74:32. doi:10.1145/3290387
- [41] Farzin Houshmand, Javad Saberlatibari, and Mohsen Lesani. 2022. Hamband: RDMA replicated data types. In *PLDI '22: 43rd ACM SIGPLAN International Conference on Programming Language Design and Implementation, San Diego, CA, USA, June 13 – 17, 2022*, Ranjit Jhala and Isil Dillig (Eds.). ACM, 348–363. doi:10.1145/3519939.3523426
- [42] Patrick Hunt, Mahadev Konar, Flavio P. Junqueira, and Benjamin Reed. 2010. ZooKeeper: Wait-free Coordination for Internet-scale Systems. In *Proceedings of the 2010 USENIX Conference on USENIX Annual Technical Conference (Boston, MA) (USENIXATC '10)*. USENIX Association, Berkeley, CA, USA, 11–11.
- [43] Stephen Ibanez, Alex Mallery, Serhat Arslan, Theo Jepsen, Muhammad Shahbaz, Changhoon Kim, and Nick McKeown. 2021. The nanoPU: A Nanosecond Network Stack for Datacenters.. In *OSDI*. 239–256.
- [44] Zsolt István, David Sidler, Gustavo Alonso, and Marko Vukolic. 2016. Consensus in a box: Inexpensive coordination in hardware. In *13th {USENIX} Symposium on Networked Systems Design and Implementation ({NSDI} 16)*. 425–438.
- [45] Joseph Izraelevitz, Gaukas Wang, Rhett Hanscom, Kayli Silvers, Tamara Silbergleit Lehman, Gregory V. Chockler, and Alexey Gotsman. 2022. Acuerdo: Fast Atomic Broadcast over RDMA. In *Proceedings of the 51st International Conference on Parallel Processing, ICPP 2022, Bordeaux, France, 29 August 2022 - 1 September 2022*. ACM, 59:1–59:11. doi:10.1145/3545008.3545041
- [46] Anuj Kalia, Michael Kaminsky, and David G. Andersen. 2019. Datacenter RPCs can be General and Fast. In *16th USENIX Symposium on Networked Systems Design and Implementation, NSDI 2019, Boston, MA, February 26–28, 2019*, Jay R. Lorch and Minlan Yu (Eds.). USENIX Association, 1–16. <https://www.usenix.org/conference/nsdi19/presentation/kalia>
- [47] Antonios Katsarakis, Vasilis Gavrielatos, M. R. Siavash Katebzadeh, Arpit Joshi, Aleksandar Dragojevic, Boris Grot, and Vijay Nagarajan. 2020. Hermes: A Fast, Fault-Tolerant and Linearizable Replication Protocol. In *ASPLOS '20: Architectural Support for Programming Languages and Operating Systems, Lausanne, Switzerland, March 16–20, 2020*, James R. Larus, Luis Ceze, and Karin Strauss (Eds.). ACM, 201–217. doi:10.1145/3373376.3378496
- [48] Mikhail Kazhemiaka, Babar Naveed Memon, Chathura Kankanamge, Siddhartha Sahu, Sajjad Rizvi, Bernard Wong, and Khuzaima Daudjee. 2019. Sift: resource-efficient consensus with RDMA. In *Proceedings of the 15th International Conference on Emerging Networking Experiments And Technologies, CoNEXT 2019, Orlando, FL, USA, December 09–12, 2019*, Aziz Mohaisen and Zhi-Li Zhang (Eds.). ACM, 260–271. doi:10.1145/3359989.3365437
- [49] Colin Ian King. 2024. Powerstat: Power Consumption Measurement Tool. <https://github.com/ColinIanKing/powerstat>. Accessed: 2024-10-18.
- [50] Marios Kogias and Edouard Bugnion. 2020. Hovocraft: achieving scalability and fault-tolerance for microsecond-scale datacenter services. In *Proceedings of the Fifteenth European Conference on Computer Systems*. 1–17.
- [51] Dario Korolija, Timothy Roscoe, and Gustavo Alonso. 2020. Do OS abstractions make sense on FPGAs?. In *14th USENIX Symposium on Operating Systems Design and Implementation (OSDI 20)*. USENIX Association, 991–1010. <https://www.usenix.org/conference/osdi20/presentation/roscoe>

- [52] Shadaj Laddad, Conor Power, Mae Milano, Alvin Cheung, Natacha Crooks, and Joseph M. Hellerstein. 2022. Keep CALM and CRDT On. *Proc. VLDB Endow.* 16, 4 (2022), 856–863. doi:10.14778/3574245.3574268
- [53] Avinash Lakshman and Prashant Malik. 2010. Cassandra: a decentralized structured storage system. *ACM SIGOPS Operating Systems Review* 44, 2 (2010), 35–40.
- [54] Leslie Lamport. 1998. The Part-time Parliament. *ACM Trans. Comput. Syst.* 16, 2 (1998).
- [55] Leslie Lamport. 2004. Generalized Consensus and Paxos. (2004).
- [56] Mihai Letia, Nuno M. Pregoica, and Marc Shapiro. 2010. Consistency without concurrency control in large, dynamic systems. *ACM SIGOPS Oper. Syst. Rev.* 44, 2 (2010), 29–34. doi:10.1145/1773912.1773921
- [57] Nicholas V Lewchenko, Arjun Radhakrishna, Akash Gaonkar, and Pavol Černý. 2019. Sequential programming for replicated data stores. *Proceedings of the ACM on Programming Languages* 3, ICFP (2019), 1–28.
- [58] Bojie Li, Zhenyuan Ruan, Wencong Xiao, Yuanwei Lu, Yongqiang Xiong, Andrew Putnam, Enhong Chen, and Lintao Zhang. 2017. KV-Direct: High-Performance In-Memory Key-Value Store with Programmable NIC. In *Proceedings of the 26th Symposium on Operating Systems Principles* (Shanghai, China) (SOSP '17). Association for Computing Machinery, New York, NY, USA, 137–152. doi:10.1145/3132747.3132756
- [59] Cheng Li, João Leitão, Allen Clement, Nuno Pregoica, Rodrigo Rodrigues, and Viktor Vafeiadis. 2014. Automating the Choice of Consistency Levels in Replicated Systems. In *Proceedings of the 2014 USENIX Conference on USENIX Annual Technical Conference* (Philadelphia, PA) (USENIX ATC '14). USENIX Association, Berkeley, CA, USA, 281–292.
- [60] Cheng Li, João Leitão, Allen Clement, Nuno Pregoica, and Rodrigo Rodrigues. 2015. Minimizing coordination in replicated systems. In *Proceedings of the First Workshop on Principles and Practice of Consistency for Distributed Data*. ACM, 8.
- [61] Cheng Li, Daniel Porto, Allen Clement, Johannes Gehrke, Nuno Pregoica, and Rodrigo Rodrigues. 2012. Making Geo-replicated Systems Fast As Possible, Consistent when Necessary. In *Proceedings of the 10th USENIX Conference on Operating Systems Design and Implementation* (Hollywood, CA, USA) (OSDI '12). USENIX Association, Berkeley, CA, USA, 265–278. <http://dl.acm.org/citation.cfm?id=2387880.2387906>
- [62] Feng Li, Sudipto Das, Manoj Yamala, and Vivek R. Narasayya. 2016. Accelerating Relational Databases by Leveraging Remote Memory and RDMA. In *Proceedings of the 2016 International Conference on Management of Data (SIGMOD 2016)*. ACM, 355–370. doi:10.1145/2882903.2882949
- [63] Xiao Li, Farzin Houshmand, and Mohsen Lesani. 2020. Hampa: Solver-Aided Recency-Aware Replication. In *Computer Aided Verification - 32nd International Conference, CAV 2020, Los Angeles, CA, USA, July 21-24, 2020, Proceedings, Part I (Lecture Notes in Computer Science, Vol. 12224)*, Shuvendu K. Lahiri and Chao Wang (Eds.). Springer, 324–349. doi:10.1007/978-3-030-53288-8\_16
- [64] Geoffrey Litt, Sarah Lim, Martin Kleppmann, and Peter van Hardenberg. 2022. Peritext: A CRDT for Collaborative Rich Text Editing. *Proc. ACM Hum. Comput. Interact.* 6, CSCW2 (2022), 1–36. doi:10.1145/3555644
- [65] Ming Liu, Tianyi Cui, Henry Schuh, Arvind Krishnamurthy, Simon Peter, and Karan Gupta. 2019. Offloading distributed applications onto smartNICs using iPipe. In *Proceedings of the ACM Special Interest Group on Data Communication, SIGCOMM 2019, Beijing, China, August 19-23, 2019*, Jianping Wu and Wendy Hall (Eds.). ACM, 318–333. doi:10.1145/3341302.3342079
- [66] Haodi Lu, Haikun Liu, Chencheng Ye, Xiaofei Liao, Fubing Mao, Yu Zhang, and Hai Jin. 2023. Software-Defined, Fast and Strongly-Consistent Data Replication for RDMA-Based PM Datastores. In *IEEE International Parallel and Distributed Processing Symposium, IPDPS 2023, St. Petersburg, FL, USA, May 15-19, 2023*. IEEE, 90–101. doi:10.1109/IPDPS54959.2023.00019
- [67] André Medeiros. 2012. *ZooKeeper's atomic broadcast protocol: Theory and practice*. Technical Report.
- [68] Sreeja S. Nair, Gustavo Petri, and Marc Shapiro. 2020. Proving the Safety of Highly-Available Distributed Objects. In *Programming Languages and Systems - 29th European Symposium on Programming, ESOP 2020, Held as Part of the European Joint Conferences on Theory and Practice of Software, ETAPS 2020, Dublin, Ireland, April 25-30, 2020, Proceedings (Lecture Notes in Computer Science, Vol. 12075)*, Peter Müller (Ed.). Springer, 544–571. doi:10.1007/978-3-030-44914-8\_20
- [69] Brian M. Oki and Barbara H. Liskov. 1988. Viewstamped Replication: A New Primary Copy Method to Support Highly-Available Distributed Systems. In *Proceedings of the Seventh Annual ACM Symposium on Principles of Distributed Computing* (Toronto, Ontario, Canada) (PODC '88). ACM, New York, NY, USA, 8–17.
- [70] Diego Ongaro and John Ousterhout. 2014. In search of an understandable consensus algorithm. In *Proceedings of the 2014 USENIX Conference on USENIX Annual Technical Conference* (Philadelphia, PA) (USENIX ATC '14). USENIX Association, USA, 305–320.
- [71] Diego Ongaro and John Ousterhout. 2014. In Search of an Understandable Consensus Algorithm. In *Proceedings of the 2014 USENIX Conference on USENIX Annual Technical Conference* (Philadelphia, PA) (USENIX ATC '14). USENIX Association, Berkeley, CA, USA, 305–320.
- [72] Seo Jin Park and John Ousterhout. 2019. Exploiting commutativity for practical fast replication. In *16th {USENIX} Symposium on Networked Systems Design and Implementation ({NSDI} 19)*, 47–64.
- [73] Fernando Pedone and André Schiper. 2002. Handling message semantics with generic broadcast protocols. *Distributed Computing* 15, 2 (2002), 97–107.
- [74] Marius Poke and Torsten Hoefler. 2015. DARE: High-Performance State Machine Replication on RDMA Networks. In *Proceedings of the 24th International Symposium on High-Performance Parallel and Distributed Computing* (Portland, Oregon, USA) (HPDC '15). Association for Computing Machinery, New York, NY, USA, 107–118. doi:10.1145/2749246.2749267
- [75] PowerTOP 2024. <https://github.com/fenrus75/powertop>.
- [76] Andrew Putnam, Adrian M. Caulfield, Eric S. Chung, Derek Chiou, Kypros Constantinides, John Demme, Hadi Esmaeilzadeh, Jeremy Fowers, Gopi Prashanth Gopal, Jan Gray, Michael Haselman, Scott Hauck, Stephen Heil, Amir Hormati, Joo-Young Kim, Sitaram Lanka, James R. Larus, Eric Peterson, Simon Pope, Aaron Smith, Jason Thong, Phillip Yi Xiao, and Doug Burger. 2014. A reconfigurable fabric for accelerating large-scale datacenter services. In *ACM/IEEE 41st International Symposium on Computer Architecture, ISCA 2014, Minneapolis, MN, USA, June 14-18, 2014*. IEEE Computer Society, 13–24. doi:10.1109/ISCA.2014.6853195
- [77] Feng Ren, Mingxing Zhang, Kang Chen, Huaxia Xia, Zuoning Chen, and Yongwei Wu. 2024. Scaling Up Memory Disaggregated Applications with SMART. In *Proceedings of the 29th ACM International Conference on Architectural Support for Programming Languages and Operating Systems, Volume 1, ASPLOS 2024, La Jolla, CA, USA, 27 April 2024 - 1 May 2024*, Rajiv Gupta, Nael B. Abu-Ghazaleh, Madan Musuvathi, and Dan Tsafir (Eds.). ACM, 351–367. doi:10.1145/3617232.3624857
- [78] Scaphandre 2024. <https://github.com/hubblo-org/scaphandre>.
- [79] Fred B. Schneider. 1990. Implementing fault-tolerant services using the state machine approach: A tutorial. *ACM Computing Surveys (CSUR)* 22, 4 (1990), 299–319.
- [80] Henry N. Schuh, Weihao Liang, Ming Liu, Jacob Nelson, and Arvind Krishnamurthy. 2021. Xenic: SmartNIC-Accelerated Distributed Transactions. In *SOSP '21: ACM SIGOPS 28th Symposium on Operating Systems Principles, Virtual Event / Koblenz, Germany, October 26-29, 2021*, Robert van Renesse and Nikolai Zeldovich (Eds.). ACM, 740–755. doi:10.1145/3477132.3483555
- [81] Marc Shapiro, Masoud Saeida Ardekani, and Gustavo Petri. 2016. *Consistency in 3D*. Ph. D. Dissertation. Institut National de la Recherche en Informatique et Automatique (Inria).
- [82] Marc Shapiro, Nuno Pregoica, Carlos Baquero, and Marek Zawirski. 2011. Conflict-free replicated data types. In *Symposium on Self-Stabilizing Systems*. Springer, 386–400.
- [83] Marc Shapiro, Nuno M. Pregoica, Carlos Baquero, and Marek Zawirski. 2011. Conflict-Free Replicated Data Types. In *Stabilization, Safety, and Security of Distributed Systems - 13th International Symposium, SSS 2011, Grenoble, France, October 10-12, 2011, Proceedings (Lecture Notes in Computer Science, Vol. 6976)*, Xavier Défago, Franck Petit, and Vincent Villain (Eds.). Springer, 386–400. doi:10.1007/978-3-642-24550-3\_29
- [84] Xiao Shi, Scott Pruett, Kevin Doherty, Jinyu Han, Dmitri Petrov, Jim Carrig, John Hugg, and Nathan Bronson. 2020. FlightTracker: Consistency across Read-Optimized Online Stores at Facebook. In *14th USENIX Symposium on Operating Systems Design and Implementation, OSDI 2020, Virtual Event, November 4-6, 2020*. USENIX Association, 407–423. <https://www.usenix.org/conference/osdi20/presentation/shi>
- [85] David Sidler, Zeke Wang, Monica Chiosa, Amit Kulkarni, and Gustavo Alonso. 2020. StRoM: Smart Remote Memory. In *Proceedings of the Fifteenth European Conference on Computer Systems (Heraklion, Greece) (EuroSys '20)*. Association for Computing Machinery, New York, NY, USA, Article 29, 16 pages. doi:10.1145/3342195.3387519
- [86] KC Sivaramakrishnan, Gowtham Kaki, and Suresh Jagannathan. 2015. Declarative Programming over Eventually Consistent Data Stores. In *Proceedings of the 36th ACM SIGPLAN Conference on Programming Language Design and Implementation* (Portland, OR, USA) (PLDI '15). ACM, New York, NY, USA, 413–424.
- [87] Yacine Taleb, Ryan Stutsman, Gabriel Antoniu, and Toni Cortes. 2018. Tailwind: Fast and Atomic RDMA-based Replication. In *2018 USENIX Annual Technical Conference, USENIX ATC 2018, Boston, MA, USA, July 11-13, 2018*, Haryadi S. Gunawi and Benjamin C. Reed (Eds.). USENIX Association, 851–863. <https://www.usenix.org/conference/atc18/presentation/taleb>
- [88] Werner Vogels. 2008. Eventually consistent. *ACM Queue* 6, 6 (2008).
- [89] Cheng Wang, Jianyu Jiang, Xusheng Chen, Ning Yi, and Heming Cui. 2017. APUS: fast and scalable paxos on RDMA. In *Proceedings of the 2017 Symposium on Cloud Computing, SoCC 2017, Santa Clara, CA, USA, September 24-27, 2017*. ACM, 94–107. doi:10.1145/3127479.3128609
- [90] Zilong Wang, Layong Luo, Qingsong Ning, Chaoliang Zeng, Wenxue Li, Xinchun Wan, Peng Xie, Tao Feng, Ke Cheng, Xiongfei Geng, Tianhao Wang, Weicheng Ling, Kejia Huo, Pingbo An, Kui Ji, Shideng Zhang, Bin Xu, Ruiqing Feng, Tao Ding, Kai Chen, and Chuanxiang Guo. 2023. SRNIC: A Scalable Architecture for RDMA NICs. In *20th USENIX Symposium on Networked Systems Design and Implementation, NSDI 2023, Boston, MA, April 17-19, 2023*, Mahesh Balakrishnan and Manya Ghobadi (Eds.). USENIX Association, 1–14. <https://www.usenix.org/>

- conference/nsdi23/presentation/wang-zilong
- [91] Xingda Wei, Rongxin Chen, Yuhao Yang, Rong Chen, and Haibo Chen. 2023. Characterizing Off-path SmartNIC for Accelerating Distributed Systems. In *17th USENIX Symposium on Operating Systems Design and Implementation, OSDI 2023, Boston, MA, USA, July 10-12, 2023*, Roxana Geambasu and Ed Nightingale (Eds.). USENIX Association, 987–1004. <https://www.usenix.org/conference/osdi23/presentation/wei-smartnic>
  - [92] Michael J. Whittaker and Joseph M. Hellerstein. 2021. Interactive checks for coordination avoidance. *VLDB J.* 30, 1 (2021), 71–92. doi:10.1007/S00778-020-00628-3
  - [93] Erfan Zamanian, Xiangyao Yu, Michael Stonebraker, and Tim Kraska. 2019. Rethinking Database High Availability with RDMA Networks. *Proc. VLDB Endow.* 12, 11 (2019), 1637–1650. doi:10.14778/3342263.3342639
  - [94] Erfan Zamanian, Xiangyao Yu, Michael Stonebraker, and Tim Kraska. 2019. Rethinking Database High Availability with RDMA Networks. *Proc. VLDB Endow.* 12, 11 (2019), 1637–1650. doi:10.14778/3342263.3342639
  - [95] Michael Zink, David Irwin, Emmanuel Cecchet, Hakan Saplakoglu, Orran Krieger, Martin Herbordt, Michael Daitzman, Peter Desnoyers, Miriam Leeser, and Suranga Handagala. 2021. The Open Cloud Testbed (OCT): A Platform for Research into new Cloud Technologies. In *2021 IEEE 10th International Conference on Cloud Networking (CloudNet)*. 140–147. doi:10.1109/CloudNet53349.2021.9657109

Table A.1: CRDTs

CRDT	State	Reducible	Irreducible
G-Counter	Scalar $C$	<i>increment</i>	
PN-Counter	Scalar $C$	<i>increment</i> <i>decrement</i>	
LWW-Register	Scalar $R$ Scalar $T$	<i>assign</i>	
G-Set	Set $S$	<i>insert</i>	
PN-Set	Array $C$		<i>insert</i> <i>remove</i>
2P-Set	Set $A$ Set $R$		<i>insert</i> <i>remove</i>

## A Conflict-free Replicated Data Types

A CRDT is a data type (or data structure) that can be replicated across in a distributed computer system in manner that provides several properties. Updates can be performed independently and concurrently at any replica; algorithms within the CRDT that are transparent to the user/programmer propagate updates to all other replicas, resolving any inconsistencies that may occur; and convergence under the strong eventual consistency model is guaranteed. It is important to note that strong eventual consistency *does not* guarantee any timeline by which convergence will be achieved.

Two different CRDT design and implementation strategies have been proposed: operation-[15, 56] and state-based [6, 16]. Both operation-based and state-based CRDTs provide strong eventual consistency, and they are theoretically equivalent, meaning that any operation-based CRDT can emulate its state-based counterpart, and vice-versa [82]. State-based CRDTs require periodic transmission of each replica’s state to other replicas, requiring a non-trivial state merge operation, depending on the level of sophistication of the CRDT. In contrast, operation-based CRDTs require each replica to broadcast each method invocation to the other replicas, which increases network communication. The CRDT Wikipedia page<sup>3</sup> provides further details.

### A.1 CRDT Benchmark Summary

The CRDTs used for experimental evaluation are described as follows. Our evaluation is limited to scalar instances of each CRDT.

**G-Counter**<sup>4</sup>: A grow-only counter, which can only be incremented.

**PN-Counter**: A positive-negative counter which supports increment and decrement operations. A PN-Counter comprises two G-Counters: one for increments, and one for decrements.

**LWW-Register**: A last writer wins register, which supports assignment of values to the register. Unique timestamps are associated with each assignment, which ensures a total order of operations. The register always retains the most recently written value.

**G-Set**: A grow-only set which supports insertion, but not removal, of set elements.

**PN-Set**: A counter is associated with each element of a set: insertion increments the counter; removal decrements the counter. An element is present in the set of its counter is positive. A PN-set may

<sup>3</sup>[https://en.wikipedia.org/wiki/Conflict-free\\_replicated\\_data\\_type](https://en.wikipedia.org/wiki/Conflict-free_replicated_data_type)

<sup>4</sup>We do not include G-Counter as a benchmark; it is a building block for the PN-Counter.

represent a non-traditional multi-set, in which a positive counter value represents the number of occurrences of an element in the set; however, when the counter becomes negative, multiple insertion operations are needed to reintroduce the element to the multi-set.

**2P-Set**: A two-phase set that supports insertion and removal of set elements. Once removed, an element cannot be reinserted into the set. A 2P-Set is typically implemented using two G-Sets.

## B Well-Coordinted Replicated Data Types

WRDTs generalize CRDTs with the addition of conflicting methods which require strong consistency [40, 41, 63]. Strong consistency necessitates an SMR protocol to synchronize conflicting calls. Like CRDTs, WRDTs provide strong eventual consistency for non-conflicting method categories. WRDTs thereby guarantee convergence for both conflicting and non-conflicting method categories. WRDTs also provide invariants which are satisfied through permissibility checks, thereby guaranteeing integrity.

### B.1 WRDT Benchmark Summary

The WRDTs used for experimental evaluation are described as follows.

**Bank Account**: A distributed bank account that maintains a scalar balance; *deposit()* and *withdraw()* methods respectively increase and reduce the balance. Withdrawals that cause overdrafts (funds less than 0) are impermissible.

**Courseware**: A university registrar that manages courses to be taught (*addCourse()*, *deleteCourse()*), enrolls students in the University (*addStudent()*), and enrolls students in courses (*enroll()*).

**Project**: Business software that manages projects (*addProject()*, *deleteProject()*), enrolls personnel (*addEmployee()*) and assigns personnel to work on projects (*assign()*).

**Movie**: A database of movies (*addMovie()*, *deleteMovie()*) and customers (*addCustomer()*, *deleteCustomer()*).

**Auction**: An e-commerce site that manages users (*registerUser()*), lists items for direct sale (*sellItem()*), allows users to purchase items (*buyItem()*), and facilitates item sales via auction (*openAuction()*, *placeBid()*, *closeAuction()*).

Bank Account’s state comprises a single scalar, i.e., one account with one balance. The other WRDTs’ states comprise two or three sets, and in the case of Auction, three sets and one array.

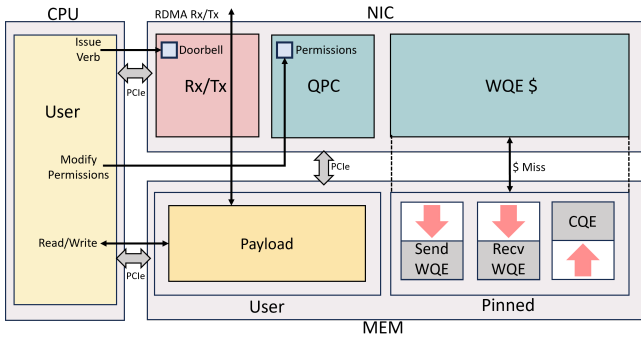
## C RDMA

RDMA was originally proposed for high-performance computing (HPC) clusters through the Infiniband protocol, and was later adapted for data center networks as RDMA over Converged Ethernet (RoCE), a link-layer protocol; RoCEv2 is implemented on top of UDP/IPv4 or UDP/IPv6 as an internet-layer protocol, which supports packet routing. Further details can be found on the RoCE Wikipedia page<sup>5</sup>.

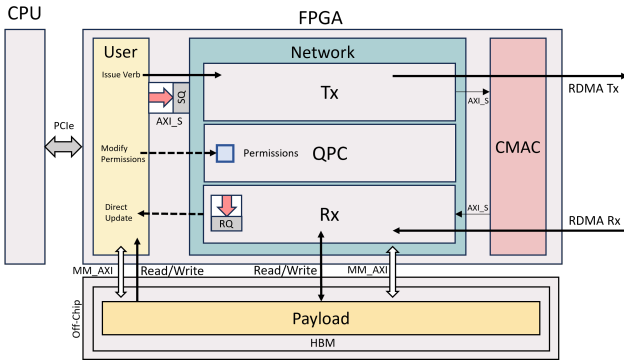
<sup>5</sup>[https://en.wikipedia.org/wiki/RDMA\\_over\\_Converged\\_Ethernet](https://en.wikipedia.org/wiki/RDMA_over_Converged_Ethernet)

Table B.1: WRDT Methods and Invariants

RDT	State	Reducible	Irreducible	Conflicting	Sync Group
Bank Account	Scalar $B$	$deposit(d)$		$withdraw(w)$ where $B - w \geq 0$	1
Courseware	Set $S$ Set $C$ Set $E$		$addStudent(s)$ where $s \notin S$	$addCourse(c)$ where $c \notin C$ $deleteCourse(c)$ where $c \in C$ $enroll(s, c)$ where $s \in S, c \in C, \langle s, c \rangle \notin E$	1
Project	Set $E$ Set $P$ Set $A$		$addEmployee(e)$ where $e \notin E$	$addProject(p)$ where $p \notin P$ $deleteProject(p)$ where $p \in P$ $assign(e, p)$ where $e \in E, p \in P, \langle e, p \rangle \notin A$	1
Movie	Set $C$ Set $M$			$addCustomer(c)$ where $c \notin C$ $deleteCustomer(c)$ where $c \in C$ $addMovie(m)$ where $m \notin M$ $deleteMovie(m)$ where $m \in M$	2
Auction	Set $U$ Set $A$ Set $I$ Array $S[]$	$sellItem(i, u)$	$openAuction(a)$ where $a \notin A$	$registerUser(u)$ where $u \notin U$ $buyItem(i, u)$ where $i \in I, S[i] \geq 1, u \in U$ $placeBid(a, bid, u)$ where $a \in A, u \in U$ $closeAuction(a)$ where $a \in A$	3



(a) Architectural components that implement RDMA for a traditional CPU-based network.



(b) RDMA architecture for a network-attached FPGA featuring a soft RNIC [85].

Figure 18: Architectural components that implement RDMA for both a CPU and FPGA.

### C.1 RDMA vs. Socket-based Networking

Figure 18 respectively depicts the components (CPU, memory, NIC) that implement socket-based and RDMA networks; both figures assume that all three components are connected via PCIe.

In Figure 18, the operating system (OS), but not the user-space application, communicates with the NIC. User-space applications must incur the overhead of system calls to transmit and receive

data. All data received by the NIC is written to memory managed by the OS kernel; once received, the OS copies data to user-space memory, before the user-space application can access the data.

In Figure 18, the user-space application communicates directly with an RDMA-enabled NIC (RNIC), bypassing the OS kernel. As the RNIC provides remote access to user-space memory, the RNIC's Queue Pair Context (QPC) assumes responsibility for managing memory access permissions, a function typically performed by the OS in other contexts. The three queues that comprise an RDMA queue-pair (QP) for each RDMA connection are allocated in a pinned memory segment. The RNIC contains a cache that provides fast access to QPs. Data is remotely written to user-space memory, eliminating the need to copy data from kernel-managed into user-space memory in Figure 18. User-space applications that expect to receive data poll their memory segments to access data written by remotely-initiated **RDMA\_Writes**, and their QPs to detect completion of locally-initiated **RDMA\_Reads**.

To refresh terminology, the QP on each side of a connection comprises three queues: a Send Queue (SQ), a Receive Queue (RQ), and a Completion Queue (CQ). The user-space application issues a work request by posting a Work Queue Entry (WQE) to the QP: a Send Queue Entry (SQE) is posted to the SQ, a Receive Queue Entry (RQE) is posted to the RQ, and a Completion Queue Entry (CQE) is posted to the CQ.

### C.2 RDMA\_READ

Figure 19 depicts the **RDMA\_Read** path for a CPU-based RDMA network. The user-application (1) posts a **SQE** and **RQE** to the SQ and RQ and (2) triggers the RNIC by writing to the doorbell register; both of these steps entail PCIe transactions and the first step accesses memory. The RNIC (3) fetches the **SQE** from memory, (4) checks the QP state, (5) verifies permissions, and (6) packages the **RDMA\_Read** operation for transmission over the network; step (4) incurs PCIe transaction and memory access latencies. On the receiving side, the RNIC (7) retrieves and unpacks that **RDMA\_Write** operation, (8) verifies permissions, and (9) reads the payload from memory over PCIe at the address specified in the operation. The receiver's RNIC (a, b) returns the payload over the network to the sender who (c) writes the received payload to memory, (d) fetches the **RQE** from the RQ and (e) writes a **CQE** to the CQ, signaling completion of the operation; steps (c), (d), and (e) incur PCIe transaction

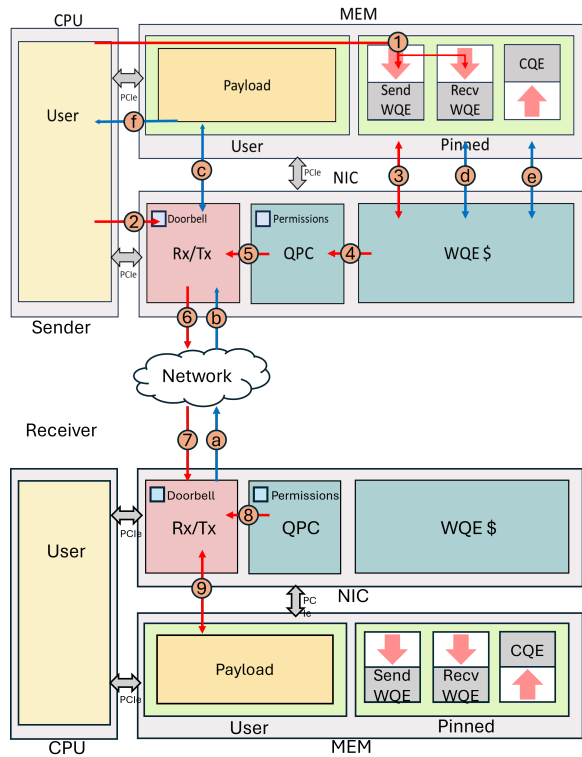


Figure 19: CPU Nic read path

and memory access latencies. The sender's user application can (f) access memory at any time to retrieve the remotely read payload.

### C.3 RDMA\_WRITE

Figure 20 depicts the **RDMA\_Write** path for a CPU-based RDMA network. The user-application (1) writes the payload intended for transmission into memory; (2) posts an *SQE* to the *SQ*; and (3) triggers the RNIC by writing to a doorbell register; all three of these steps entail PCIe transactions, and the first two access memory. The RNIC (4) fetches the *SQE* from memory, (5) checks the QP state, (6) verifies permissions and packet header information, (7) retrieves the payload from memory, and (8) packages the **RDMA\_Write** operation for transmission across the network; steps (4) and (7) incur PCIe transactions and memory access latencies. On the receiving side, the RNIC (9) retrieves and unpacks the **RDMA\_Write** operation, (10) verifies permissions, and (11) writes the payload to memory over PCIe. The receiver's RNIC (a, b) returns an acknowledgment (ACK) to the sender, whose RNIC completes the **RDMA\_Write** operation by posting a CQE to the CQ. The receiver's user application can (12) access memory at any time to retrieve the remotely written payload.

### C.4 RDMA\_READ (FPGA Implementation)

Figure 21 depicts the **RDMA\_Read** path for a pair of network-attached FPGAs.

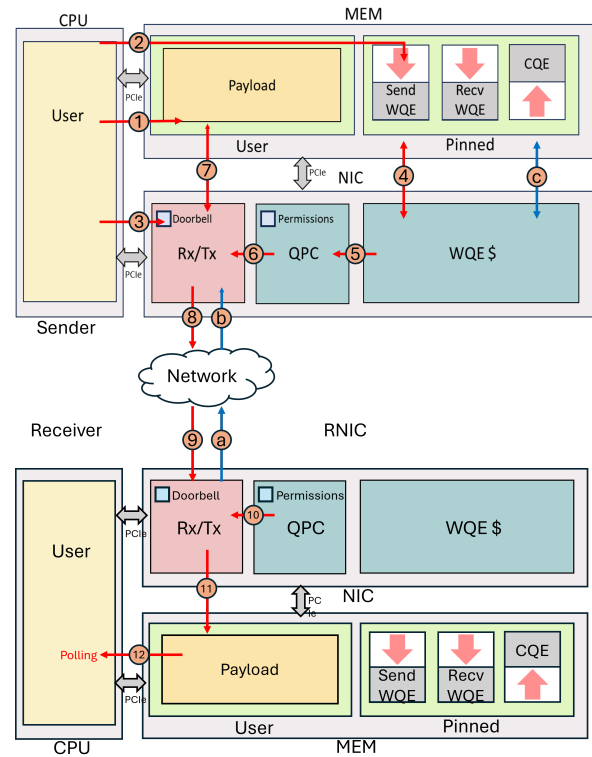


Figure 20: CPU Nic write path

The user kernel (1) pushes the **RDMA\_Read** operation to the *SQ*, implemented as a AXI Stream interface. (2) The Network kernel pops the verb from the *SQ* and (3) checks the *QPC* for permissions, and connection information. Since the operation is **RDMA\_Read**, (4) an *RQE* is posted to the *RQ*, which resides in on-chip BRAM. The RDMA packet is (5) packaged and transferred to the CMAC through an AXI Stream. The CMAC takes the RDMA packet, adds Ethernet headers, and (6, 7) transmits the packet over the network. At the receiving node, the CMAC strips the Ethernet header and (8) passes the RDMA packet to the Network kernel. The remote Network kernel (9) checks permissions, and (10) issues the read operation to memory through a memory-mapped AXI interface to obtain the payload, and (a) passes the payload to the network kernel for transmission back to the node that initiated the verb. The RDMA packet is (b, c, d) returned and (e) received by the Network kernel. The Network kernel (f) pops the *RQE* from the *RQ* and writes the payload to the requested address in memory. The User kernel (g) accesses the payload through a memory-mapped AXI interface.

### C.5 RDMA\_WRITE (FPGA Implementation)

Figure 22 depicts the **RDMA\_Write** path for a pair of network-attached FPGAs.

The user kernel (1) pushes the **RDMA\_Write** verb to the *SQ*, implemented as a AXI Stream interface. (2) The Network kernel pops the verb from the *SQ* and (3) checks the *QPC* for permissions, and connection information. The Network kernel maintains

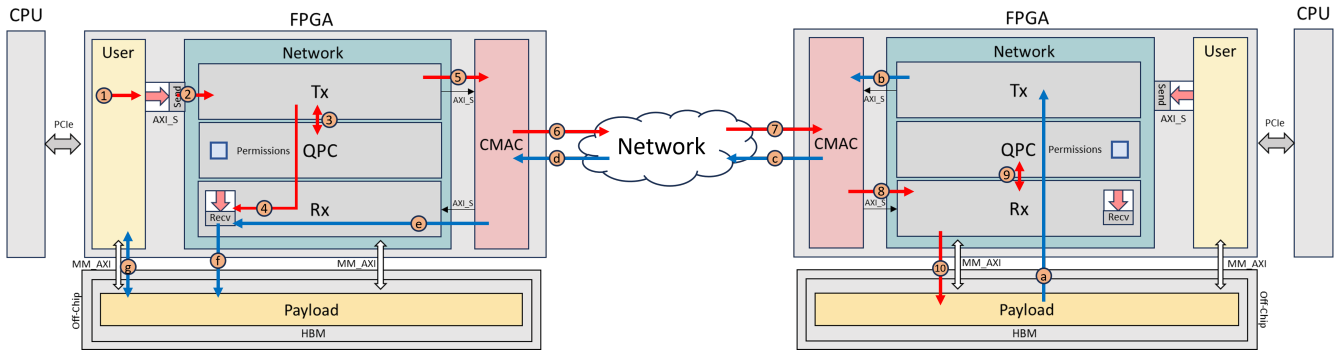


Figure 21: FPGA RDMA read path

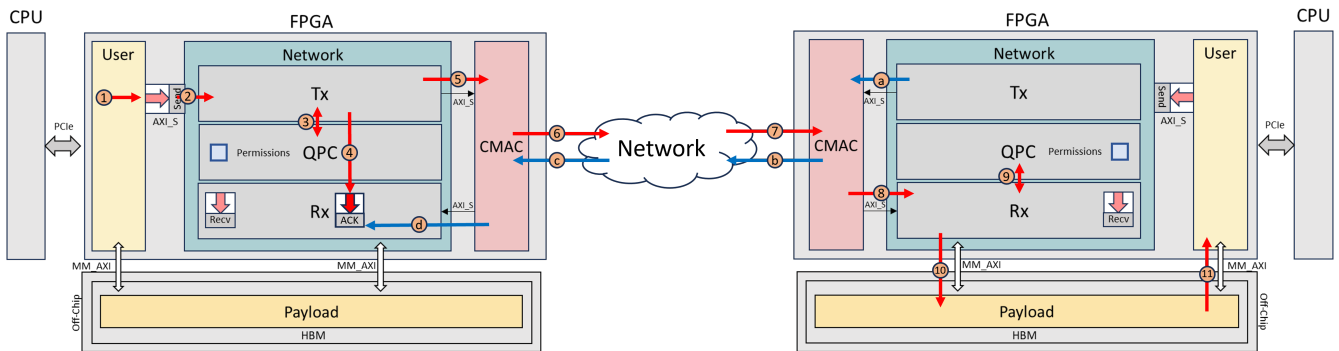


Figure 22: FPGA RDMA write path

an queue of expected acknowledgments (ACKs) for retransmission purposes; before transmitting an RDMA packet, the Network kernel posts an expected ACK into the ACK queue. The RDMA packet is (5) packaged and transferred to the CMAC through an AXI Stream. The CMAC takes the RDMA packet, adds Ethernet headers, and (6, 7) transmits the packet over the network. At the receiving node, the CMAC strips the Ethernet header and (8) passes the RDMA packet to the Network kernel. The remote Network kernel (9) checks permissions, and (10) writes the payload to memory through a memory-mapped AXI interface. The User kernel (11) can then access the payload through its own memory-mapped AXI interface. The receiving node generates an ACK and (a) transmits to the CMAC and (b, c) across the network. The sender receives the ACK, notifying it that the **RDMA\_Write** verb successfully completed. The Network kernel (d) removes the expected ACK from the ACK queue, thereby completing the operation.

### C.6 FPGA-Specific RDMA Verbs.

Read and Write verbs communicate with remote CPUs via host memory<sup>6</sup>. An analogous implementation of these verbs on a network-attached FPGA utilizes HBM as an intermediary between the local User kernel and the remote node [85] (23).

In 23, we propose RDMA verbs specialized for network-attached FPGAs. Modern FPGAs provide integrated storage. For example,

<sup>6</sup>RDMA does not support direct access to the CPU register file or cache hierarchy.

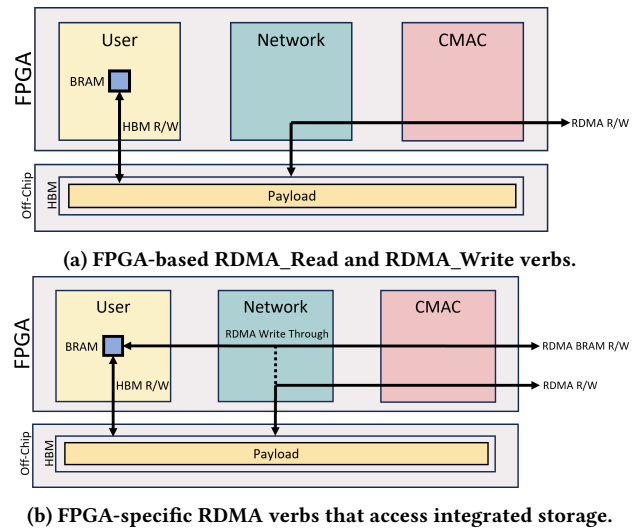
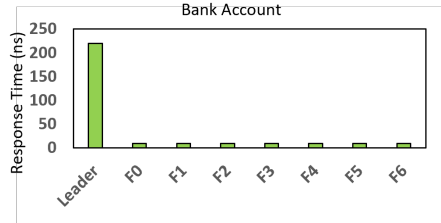


Figure 23: RDMA verbs for network-attached FPGAs.

the AMD Ultrascale FPGA in the Alveo U280 accelerator card integrates 2,607,000 registers, 2,016 *Block RAMs* (BRAMs) (36 Kb each)

**Table C.1: Average latencies measured for several RDMA verbs that write to FPGA integrated storage.**

Operation	Latency
Write	413 ns
BRAM_Write	309 ns
BRAM_Write_Through	309 ns
Register_Write	285 ns
Register_Write_Through	285 ns

**Figure 24: Execution time of all replicas for Bank Account WRDT in a 15% write percentage 8-Node configuration**

and 960 *UltraRAMs* (288 Kb each); plus any portion of the programmable fabric can be configured as storage. Our proposed FPGA-specific RDMA verbs can read or write to these resources, along with Write-Through verbs which concurrently write to integrated storage and HBM.

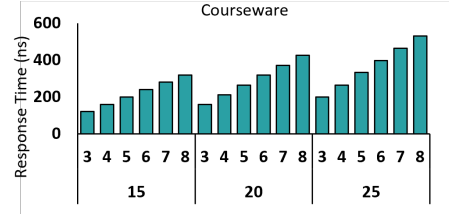
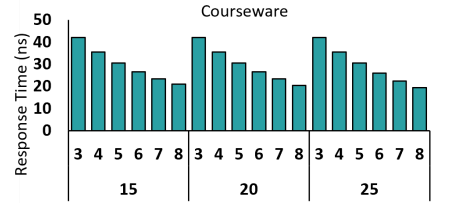
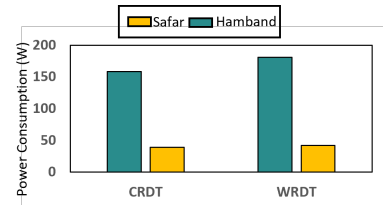
Table C.1 reports the latencies of some Write and Write-Through verbs that write to FPGA integrated storage resources. The reported latencies include network transmission, RDMA stack, and HBM, BRAM, or register access latencies. In the case of the Write-Through verbs, the time reported is for BRAM, and a register. Table C.1 *does not* report the time to generate and receive ACKs. We identify one RDT use-case for a write-through verb (subsection 4.3).

## D Experiments

### D.1 Bank Account: Leaders vs Followers

Figure 24 reports the execution time of the Bank Account WRDT with 8 replicas and a write percentage of 15%. The Leader’s execution time is more than twice as larger as the execution times of the seven follower replicas F0-F6; the follower execution times are approximately equal. Throughput is defined as the total execution time of the workload divided by the total execution time of the system. The total execution time is constrained by the longest-running replica, which is the Leader in Figure 24. Presuming that Bank Account is representative of all WRDTs, Figure 24 indicates that the most promising way to improve throughput is to improve the performance of the Leader, which means focusing on how conflicting transactions and coordination are implemented.

Figure 25 reports the leader execution times across 3-8 replicas and write percentages of 15%, 20%, and 25%, for the Courseware WRDT. Increasing the write percentage tends to increase leader execution time, since there are more conflicting transactions. To recall, the write percentage is the fraction of methods that write state, which includes reducible, irreducible conflict-free, and conflicting methods, whereas, all remaining calls invoke the *query()* method. Increasing the number of replicas tend to increase leader

**Figure 25: Execution time of leaders in Courseware WRDT****Figure 26: Execution time of followers in Courseware WRDT****Figure 27: Power Consumption**

execution time, due to the increased cost of coordinating a larger number of followers.

Conversely, Figure 26 reports the average execution time of all followers across the same range of replicas and write percentages. As the number of replicas increase, each follower invokes fewer calls, which reduces execution time. Increasing the write percentage marginally increases execution by adding more conflict-free transactions to execute; as conflict-free methods lack coordination, the slow down is minimal. Conflicting calls do not impact follower execution time to the same extent that they impact leader execution time.

### D.2 Power Consumption

FPGA power consumption was measured following AMD Xilinx Documentation [7]. CPU System power consumption was measured using *powerstat*[49].

Figure 27 reports the peak power consumption of CRDTs and WRDTs averaged across use cases and write percentages. SafarDB’s power consumption includes the entire Alveo U280 card’s power, while Hamband’s is the full system including CPU, RNIC, and memory. SafarDB consumes about 1/4th the power of Hamband while providing improved performance; this type of disparity is expected for FPGAs due to a number of reasons, including lower operating frequency and the elimination of inefficiencies such as fetching

and decoding machine instructions, data transfer up and down the

memory hierarchy on the granularity of cache lines, and the need for every arithmetic operation to access the register file [28, 38].